


# Mechanisms restraining break-induced replication at two-ended DNA double-strand breaks

Nhung Pham<sup>1</sup> , Zhenxin Yan<sup>1</sup>, Yang Yu<sup>1</sup>, Mosammat Faria Afreen<sup>2</sup>, Anna Malkova<sup>3</sup>, James E Haber<sup>2</sup> & Grzegorz Ira<sup>1,\*</sup>

## Abstract

DNA synthesis during homologous recombination is highly mutagenic and prone to template switches. Two-ended DNA double-strand breaks (DSBs) are usually repaired by gene conversion with a short patch of DNA synthesis, thus limiting the mutation load to the vicinity of the DSB. Single-ended DSBs are repaired by break-induced replication (BIR), which involves extensive and mutagenic DNA synthesis spanning up to hundreds of kilobases. It remains unknown how mutagenic BIR is suppressed at two-ended DSBs. Here, we demonstrate that BIR is suppressed at two-ended DSBs by proteins coordinating the usage of two ends of a DSB: (i) ssDNA annealing proteins Rad52 and Rad59 that promote second end capture, (ii) D-loop unwinding helicase Mph1, and (iii) Mre11-Rad50-Xrs2 complex that promotes synchronous resection of two ends of a DSB. Finally, BIR is also suppressed when Sir2 silences a normally heterochromatic repair template. All of these proteins are particularly important for limiting BIR when recombination occurs between short repetitive sequences, emphasizing the significance of these mechanisms for species carrying many repetitive elements such as humans.

**Keywords** break-induced replication; double-strand break; DSB end resection; homologous recombination; ssDNA annealing

**Subject Category** DNA Replication, Recombination & Repair

**DOI** 10.15252/embj.2020104847 | Received 27 February 2020 | Revised 4 March 2021 | Accepted 9 March 2021 | Published online 12 April 2021

**The EMBO Journal (2021) 40: e104847**

## Introduction

Two-ended double-strand breaks (DSBs) are repaired by either non-homologous end-joining (NHEJ) or homologous recombination (HR). In the most basic HR pathway by gene conversion, one of the DSB ends invades the homologous template, forming a displacement loop (D-loop) that primes short-patch new DNA synthesis. Repair is completed when the newly synthesized strand is unwound and anneals to the second end of the DSB leading to conservative

inheritance of newly synthesized strands (Ira *et al.*, 2006) (Fig 1A). This mechanism, called synthesis-dependent strand annealing (SDSA), is used in mitotically growing cells. Alternatively, the second end of a DSB anneals to the extended D-loop leading to the formation of a double Holliday junction (dHJ), an intermediate common in meiotic recombination and essential for crossover outcomes (Symington *et al.*, 2014). In repair of one-ended DSBs or when homology within the genome is present only for one end of the DSB, the single end invades the template and initiates extensive repair-specific DNA synthesis that can reach even the end of the chromosome. This pathway, called break-induced replication (BIR), proceeds via D-loop migration and leads to conservative inheritance of the newly synthesized strands (Fig 1A) (Donnianni & Symington, 2013; Saini *et al.*, 2013). Both SDSA and BIR lead to a significant increase of point mutations along the entire length of new DNA synthesis (McGill *et al.*, 1989; Ponder *et al.*, 2005; Hicks *et al.*, 2010; Deem *et al.*, 2011; Shee *et al.*, 2012; Saini *et al.*, 2013; Sakofsky *et al.*, 2014); however, the mutation load is far greater in BIR because of the increased length of repair-specific and low-fidelity DNA synthesis. In addition, frequent template switches are common in BIR within the first 10 kb of the strand invasion site (Smith *et al.*, 2007; Anand *et al.*, 2014; Stafa *et al.*, 2014). The increase of point mutations during DSB repair is attributed to the exposure of long single-strand DNA (ssDNA). Exposed ssDNA is prone to mutagenesis, and unwinding of the newly synthesized strand from its template decreases mismatch repair efficiency (Saini *et al.*, 2013; Sakofsky *et al.*, 2014). The frequent template switches in BIR are likely due to the intrinsic instability of the D-loop intermediate (Smith *et al.*, 2007; Piazza *et al.*, 2019). In diploids, the extensive use of BIR poses a threat to genome integrity by creating new mutations, template switches, and the loss of heterozygosity. In both diploids and haploids, BIR also generates nonreciprocal translocations by template switching between dispersed homologous repeats (Anand *et al.*, 2014). In humans, BIR is less characterized; but similar to yeast, extensive repair-specific DNA synthesis depends on POLD3 (yeast Pol32) and PIF1 (yeast Pif1), and conservative inheritance of newly synthesized DNA was observed during telomere recombination and during mitotic DNA synthesis (MiDAS) that likely proceeded by BIR (Lydeard *et al.*, 2007; Costantino *et al.*, 2013; Wilson *et al.*, 2013; Bhowmick *et al.*, 2016; Roumelioti *et al.*, 2016; Macheret *et al.*, 2020; Li *et al.*, 2021). Moreover, BIR and the

<sup>1</sup> Department of Molecular and Human Genetics, Baylor College of Medicine, Houston, TX, USA

<sup>2</sup> Department of Biology, Rosenstiel Basic Medical Sciences Research Center, Waltham, MA, USA

<sup>3</sup> Department of Biology, University of Iowa, Iowa City, IA, USA

\*Corresponding author. Tel: +1 713 798 1017; E-mail: gira@bcm.edu

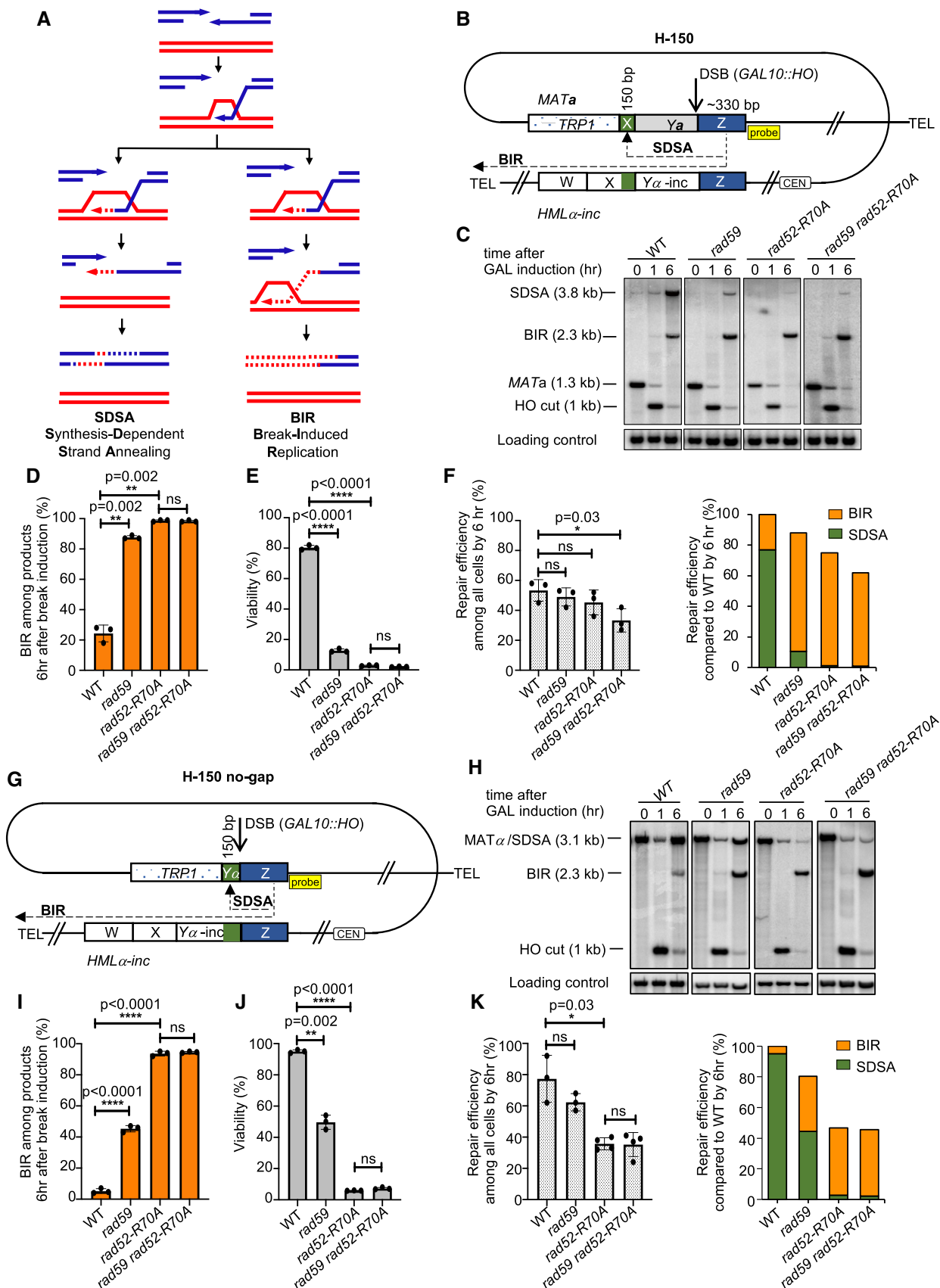


Figure 1.

**Figure 1. Role of Rad59 and DNA binding domain of Rad52 in suppressing BIR at two-ended DSBs.**

- A Models of DSB repair by SDSA and BIR.
- B Schematic of the H-150 assay. Blue boxes depict homologous sequence on one end of the DSB and green boxes depict homology on the other end. A DSB is induced at modified *MATa* locus (Chr. III). Strand invasion occurs within the “Z” sequence (blue box) and after copying  $\gamma$ -inc (dashed line) and X sequence (150 bp), the X sequence is used to capture the second end during SDSA. When copying continues to the end of chromosome via BIR (dashed line), an acentric chromosome forms and an unrepaired chromosome segment remains, leading to cell death.
- C Representative Southern blots showing DSB repair products in WT, *rad59Δ*, *rad52-R70A*, and *rad59Δ rad52-R70A* cells. DNA was digested with *Bsp1286I* and probed with a *MAT*-distal sequence (yellow box in panel B). A detailed map of restriction cut sites and expected size for different repair products are illustrated in Appendix Fig S1.
- D Percentage of BIR products among repair outcomes by 6 h are shown. (Mean  $\pm$  SD; *n* = 3).
- E Viability of indicated strains is shown (mean  $\pm$  SD; *n* = 3).
- F Graph shows repair efficiency among all cells by 6 h (left) and represents the sum of DSB repair by BIR and SDSA compared to the uncut parental band at 0 h (mean  $\pm$  SD; *n* = 3). Graph shows repair by BIR and SDSA at 6 h after break induction in mutant cells compared to repair products in WT, which are set to 100% (right).
- G Schematic of H-150 no-gap assay, where 150 bp of  $\gamma$  homology on the second end of the break is immediately adjacent to the break site.
- H Representative Southern blots showing DSB repair products in indicated mutants in H-150 no-gap assay.
- I Percentage of BIR product among all repair products by 6 h are shown. (Mean  $\pm$  SD; *n* = 3).
- J Viability of indicated strains (mean  $\pm$  SD; *n* = 3).
- K Graphs showing repair efficiency compared to uncut parental band (left) (mean  $\pm$  SD; *n*  $\geq$  3) or compared to the repair products in WT (right) at 6 h after DSB induction. See Fig 1F legend for details.

Data information: Welch’s unpaired *t*-test was used to determine the *P*-value in all panels. Source data are available online for this figure.

related microhomology-mediated BIR (MMBIR) is likely the mechanisms underlying many forms of genome instability in mammalian cells (Lee *et al*, 2007; Hastings *et al*, 2009; Carvalho *et al*, 2013; Sakofsky *et al*, 2015; Li *et al*, 2020). At least some of the nonrecurrent structural variations that involve large copy number gains are accompanied by hypermutations, implicating BIR as the mechanism (Beck *et al*, 2019).

How cells limit the use of BIR in repair of two-ended breaks is not well understood. When homology on one of two ends of a DSB is short (46–150 bp), BIR contributes to or even outcompetes SDSA (Malkova *et al*, 2005; Mehta *et al*, 2017). Also, elimination of the D-loop destabilizing enzyme Mph1, (Sun *et al*, 2008; Prakash *et al*, 2009; Stafa *et al*, 2014; Piazza *et al*, 2019), likely stabilizes D-loops, resulting in increased BIR outcomes, at least when homology is short (Mehta *et al*, 2017). Consistently, BIR is suppressed when Mph1 is overexpressed (Luke-Glaser & Luke, 2012; Stivison *et al*, 2020).

Here, we hypothesized that enzymes ensuring coordination of the usage of two DSB ends in repair may prevent BIR. Proteins important for annealing, D-loop unwinding, initial resection, and maintaining two DSB ends together were examined in this study. Annealing of ssDNA in yeast is mediated by Rad52 and Rad59 (Mortensen *et al*, 1996; Sugiyama *et al*, 1998). Both purified enzymes show annealing activity, but only Rad52 can anneal complementary ssDNA in the presence of RPA (Petukhova *et al*, 1999; Wu *et al*, 2006). Rad59 interacts with Rad52 and stimulates the annealing activity of Rad52 in suboptimal conditions, likely by mitigating the negative impact of Rad51 binding to Rad52 on ssDNA annealing (Davis & Symington, 2001; Wu *et al*, 2008; Gallagher *et al*, 2020). In cells, Rad52 is required for single-strand annealing, whereas Rad59 seems to be particularly important for annealing of shorter and not completely homologous sequences (Sugawara *et al*, 2000). Purified yeast or human Rad52 mediates second end capture to an extended joint molecule (McPherson *et al*, 2004; McIlwraith *et al*, 2005; Sugiyama *et al*, 2006; McIlwraith & West, 2008; Nimonkar *et al*, 2009). Analysis of recombination intermediates in meiosis also supports the later role of Rad52-mediated annealing in both crossover and noncrossover pathways (Lao *et al*, 2008).

Here, we tested whether the elimination of the annealing activity, that is required for the second end capture to form double Holliday junctions or to complete SDSA, can unleash BIR during repair of two-ended breaks. Besides the role of “annealases” in controlling BIR during repair of two-ended DSBs, we also tested the possible function of Mph1 which disrupts the extended D-loop in the SDSA pathway (Sun *et al*, 2008; Prakash *et al*, 2009), and the Mre11-Rad50-Xrs2 complex (MRX) responsible for initial end resection (reviewed in (Symington, 2016)) and maintaining two ends of a DSB together (Kaye *et al*, 2004; Lobachev *et al*, 2004). Finally, we examined the effect of the chromatin state of the donor template on the competition between BIR and SDSA. Multiple intra- and interchromosomal DNA recombination assays with a broad range of homology sizes (150 bp to over 100 kb) were used to test the function of these enzymes in the competition between SDSA and BIR.

## Results

### Rad59- and Rad52-mediated ssDNA annealing suppresses BIR during repair of DSB

Initial steps of both SDSA and BIR involve strand invasion of one DSB end that results in formation of a displacement loop (D-loop). Gene conversion via SDSA is completed when the D-loop is extended, and the newly synthesized strand is displaced from its template and anneals to the second DSB end (Fig 1A). In BIR, the D-loop migrates even to the end of the chromosome, creating initially a long ssDNA strand that is then converted into a double-stranded product (Saini *et al*, 2013). Previous work showed that 46, 50 bp, or even 150 bp homology on the second end is too short for efficient second end capture and for completion of SDSA, resulting in high level of BIR (Deem *et al*, 2008; Mehta *et al*, 2017). In these ectopic recombination assays, an additional potential impediment for second end capture was the presence of ~700 bp non-homologous gap between homologous sequences (Mehta *et al*, 2017). Here, we have used a number of new assays with much longer homology

ranging from 150 bp to over 100 kb, and assays with or without the gap to study the role of proteins mediating annealing and other enzymes in the competition between SDSA and BIR for DSB repair. We hypothesized that decreased annealing activity would prevent the completion of gene conversion and allow the D-loop to extend further to finish the repair by BIR.

To test the role of ssDNA annealing in the choice of repair pathway between BIR and SDSA at two-ended DSBs, a separation-of-function mutant *rad52-R70A* was introduced. This mutant is severely defective in DNA binding and ssDNA annealing, but capable of loading Rad51 properly to initiate strand exchange (Shi *et al*, 2009). Additionally, *rad59Δ* and *rad59Δ rad52-R70A* double mutants were constructed. All these mutants were previously shown to reduce the SSA repair pathway which relies entirely on ssDNA annealing (Ivanov *et al*, 1996; Mortensen *et al*, 1996; Sugiyama *et al*, 1998; Petukhova *et al*, 1999; Davis & Symington, 2001; Wu *et al*, 2006; Gallagher *et al*, 2020).

We initially used a previously developed assay, a modified intra-chromosomal mating-type switching to study competition between SDSA and BIR (Mehta *et al*, 2017). A DSB is induced by HO endonuclease at the *MATa* locus and repaired by recombination with an *HMLα-inc* template, the resulting *MATα-inc* product is not cleaved by HO endonuclease. The second template for mating-type switching, *HMRa*, was deleted. The difference between native *MAT* switching and this recombination assay is that the homology size of the second DSB end is shortened from ~1,400 bp to 150 bp (H-150 assay) (Fig 1B). The successful capture of the short second end leads to gene conversion of *MATa* to *MATα-inc* and produces viable colonies. In the event that the second end is not captured, DNA synthesis via migrating D-loop (BIR) continues to the end of the chromosome (12 kb distance), including an apparent crossover: *HML/MATα-inc*. The BIR product is inviable, as BIR forms an acentric chromosome fragment and leaves unrepaired the chromosome fragment carrying the centromere. SDSA and BIR products can be distinguished by different restriction fragment sizes on a Southern blot (Fig 1C). A detailed map of restriction cut sites and expected sizes for different repair products (BIR, SDSA, and crossovers) are illustrated in Appendix Fig S1. We note that crossovers accompanying gene conversion do not contribute to repair in this assay, because we do not observe the reciprocal crossover product. As previously shown in this H-150 assay in wild-type cells, SDSA dominated with ~82% contribution to DSB repair, with the remaining 18% being BIR products. Eliminating Rad59 reduced the contribution of the SDSA pathway to ~13%, while in *rad52-R70A* or *rad59Δ rad52R70A* mutants, SDSA was further reduced to ~1% (Fig 1C and D). We note that while an important role of Rad59 and Rad52R70 in SDSA was shown previously, the contribution of BIR had not been tested (Bai *et al*, 1999). A switch to BIR is consistent with a marked decrease in the mutants' viability, as BIR is a lethal event in this assay (Fig 1E). However, not all SDSA events were channeled to BIR in the annealing mutants, as overall product formation (BIR + SDSA) 6 h after break induction was decreased when compared to wild-type cells (Fig 1F). This finding suggests that either BIR is decreased or delayed in annealing mutants, or that short 150 bp homology on the second end interferes with BIR. Both of these possibilities are tested below.

Besides the well-established role of Rad52 in loading Rad51 and ssDNA annealing, Rad52 and its DNA-binding domain also

negatively regulate extensive resection, particularly in fission yeast (Yan *et al*, 2019). It is unlikely that the role of Rad52 in resection suppresses BIR, because the *rad52-R70A* mutant shows only a minor increase in the rate of extensive resection, much less than that observed in the equivalent fission yeast DNA-binding mutant *rad52-R45A* (Appendix Fig S2A and Yan *et al*, 2019). Second, the deletion of *DOT1* that causes a ~2-fold increase in extensive resection rate (Chen *et al*, 2012) does not alter SDSA/BIR contribution to DSB repair (Appendix Fig S2B). Finally, we note that in *rad52Δ* or *rad51Δ* strains, no repair by BIR or SDSA was observed (Appendix Fig S2C).

In the mating-type switching assay and its derivative H-150 (Fig 1B), the *Ya* sequence is replaced by *Yα-inc*. Because the *Ya* sequence is non-homologous with the template, the invading strand must synthesize across about 700-bp *Yα-inc* gap to reach 150 bp homology with the second end. It is possible that this gap and/or the non-homologous tail on the resected DSB end interferes with engaging the second end in recombination. To eliminate these constraints, we tested recombination between an *HMLα-inc* and truncated *MATα*, where only 150 bp of *Yα* remains to the left of the DSB. In this assay, homology is present immediately at both DSB ends (H-150 no-gap assay, Fig 1G, Appendix Fig S1). In wild-type cells, SDSA dominated with > 95% of total DSB repair, while in annealing-defective *rad59Δ* and *rad52-R70A* mutants, SDSA dropped to ~55 and 1%, respectively, while BIR increased (Fig 1H–K). The double mutant *rad59Δ rad52-R70A* showed a similar phenotype as the *rad52-R70A* single mutant. Similar to the H-150 assay, the overall repair efficiency decreased in annealing mutants (Fig 1K). Together, these results confirm that annealing activity suppresses BIR at DSBs with short homology, either with or without a non-homologous gap between homologous sequences. By comparing results obtained in H-150 assays with or without the gap, we also conclude that the gap and/or the presence of a non-homologous tail likely interfere with the second end capture in SDSA and therefore increase the usage of BIR, at least when homology on the second end is short (Appendix Fig S3).

### BIR mildly decreases in annealing-defective mutants

To test whether BIR itself is affected by any of the annealing mutations, we constructed a new system, called H-0, where all homology to *HMLα-inc* on the second end of the break was eliminated (Fig EV1A). As confirmed by Southern blot, BIR is the sole pathway of DSB repair and cells do not survive, as BIR is lethal in this system (Fig EV1B and C). In annealing-defective *rad52-R70A* mutant strain, we observed a decrease of BIR product formation 6 h after DSB induction to ~60% of the wild-type levels (Fig EV1D). Again, the double mutant *rad59Δ rad52-R70A* showed a similar phenotype as *rad52-R70A* single mutant. These results suggest that BIR tested here is mildly deficient in annealing-defective mutants.

In the H-0 assay, while there is no homology on the second end of the break, the homology on the invading end is also limited to ~300 bp. We therefore tested the role of annealing in the BIR assay where the invading end has no homology constraint. We employed an established BIR assay that involves recombination between a truncated and a complete chromosome III, where one DSB end has an extensive homology (~200 kb) with the template but the centromere-distal end shares only 46 bp homology (Fig EV2A) (Malkova

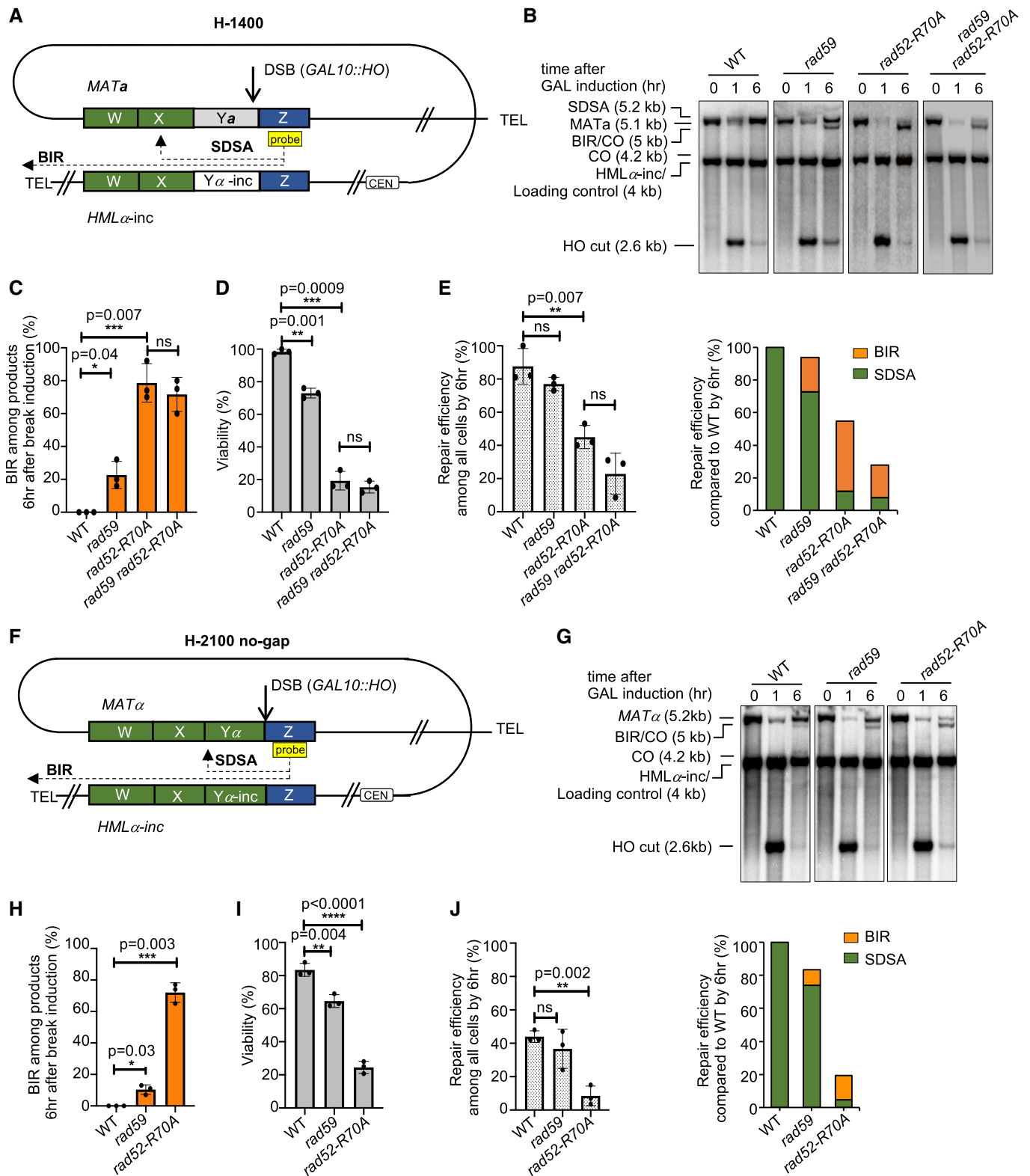


Figure 2.

**Figure 2. Rad52 and Rad59 suppress BIR during MAT switching.**

- A Schematic of the H-1400 assay. A DSB is induced at *MATa* and repaired by recombination with *HMLα-inc*. There is ~1,400 bp homology between *MATa* and *HMLα-inc* sequences on the second end (green box).
- B Representative Southern blots showing DSB repair products in WT, *rad59Δ*, *rad52-R70A*, and *rad59Δ rad52-R70A* cells. DNA was digested with *XhoI* and *EcoRI* and probed with a Z sequence (yellow box). A detailed map of restriction cut sites and expected size for different repair products are illustrated in Appendix Fig S1.
- C Percentage of BIR among all repair products by 6 h (mean ± SD; *n* = 3).
- D Viability of indicated strains (mean ± SD; *n* = 3).
- E Graphs show analysis of repair efficiency compared to uncut parental band (left) (mean ± SD; *n* = 3) and repair efficiency compared to WT (right) at 6 h after DSB induction (right). See Fig 1F for details.
- F Schematic of the H-2100 no-gap assay. A DSB is induced at *MATα* and repaired by recombination with *HMLα-inc*. There is ~2,100 bp homology between *MATα* and *HMLα-inc* sequences on the second end (green box).
- G Representative Southern blots showing DSB repair products in WT, *rad59Δ*, and *rad52-R70A*. DNA was digested with *XhoI* and *EcoRI* and probed with a Z sequence (yellow box). A detailed map of restriction cut site and expected size for different repair products are illustrated in Appendix Fig S1.
- H Percentage of BIR product among repair products by 6 h are shown (mean ± SD; *n* = 3).
- I Viability of indicated strains (mean ± SD; *n* = 3).
- J Graphs show analysis of repair efficiency compared to uncut parental band (left) (mean ± SD; *n* = 3) and repair efficiency compared to WT (right) at 6 h after DSB induction (right). See Fig 1F for details.

Data information: Welch's unpaired t-test was used to determine the *P*-value in all panels. \**P*-value 0.01 to 0.05, significant; \*\**P*-value 0.001 to 0.01, very significant; \*\*\**P*-value 0.0001 to 0.001, extremely significant; \*\*\*\**P* < 0.0001, extremely significant; *P* ≥ 0.05, not significant (ns).

*et al*, 2005). In this disomic system, there was no loss of viability after HO induction in the mutant strains. Approximately 80% of the wild-type cells use BIR for repair, during which the break end with extensive homology invades into the homologous chromosome and copies over 100 kb to the end of the chromosome. The remaining cells use the short homologous sequence at the second DSB end to complete the repair by SDSA. BIR and SDSA products can be followed by the presence of *ADE1* markers and resistance to G418 (*KANMX* marker). Consistent with previous assays, *rad52-R70A* or *rad59Δ rad52-R70A* derivatives nearly eliminated SDSA among the products (< 1%) while BIR increased to about 90% (Fig EV2B). Notably, overall DSB repair by BIR is more efficient in this assay when compared to the H-0 assay, as only 6–8% of the *Rad52-R70A* mutant cells lacking strand annealing activity failed to repair the break, resulting in chromosome loss. Thus, with much longer homology available to the invading strand, the Rad52 DNA binding domain is nearly dispensable for the completion of BIR.

One possible function of the DNA binding domain of Rad52 in BIR when homology is short could be related to the stability of the initial D-loop. Annealases related to Rad52, such as RecT or λ beta, were shown to promote three-strand exchange (Hall & Kolodner, 1994; Li *et al*, 1998), an activity that could extend the heteroduplex DNA. Alternatively, Rad52 could anneal a 3' invading strand dissociated from its template back to the disrupted - but still RPA-bound - D-loop (Fig EV1G). Interestingly, deletion of *Mph1*, a D-loop disrupting helicase, slightly increased BIR efficiency in the *rad52-R70A* strain in the H-0 assay, although not to WT levels (Fig EV1E and F). Thus, annealing activity may counteract *Mph1* by stabilizing the D-loop, at least when strand invasion is within short homologous sequences. A model presenting possible functions of Rad52's DNA binding domain in BIR is summarized in Fig EV1G.

**Rad59- and Rad52-mediated annealing suppresses BIR at DSBs in regular MAT switching**

The above BIR/SDSA competition assays had only 46–150 bp homology on the second DSB end. To test the role of annealing in a system with longer homology, we investigated regular *MAT* switching, between *MATa* and *HMLα-inc*. Here, the homology on the second end is ~1,400 bp (strain H-1400) (Fig 2A). Southern blot

analysis demonstrates that wild-type cells are nearly 100% efficient in repair, and neither BIR nor crossover contributes to repair. However, annealing-deficient mutants *rad59Δ* and particularly *rad52-R70A* increased BIR to ~30% and 60–70%, respectively (Fig 2B and C). As expected, viability is significantly reduced in annealing mutants due to a switch to lethal repair by BIR and inability to complete SDSA (Fig 2D). These results also demonstrate the importance of the optimal annealing mediated by Rad59 for the very fundamental event in yeast's life cycle, mating-type switching.

To eliminate the possible constraint of the gap and the non-homologous *Ya* tail, we tested recombination between *MATα* and *HMLα-inc* where there is no Y sequence heterology (Fig 2F). In this case, the homology on the second end is further increased to 2,100 bp (H-2100 no-gap) and is immediately next to the break. As these are *MATα* cells expressing *Mata2*, the *cis*-acting recombination enhancer (RE) that facilitates repair in *MATa* cells is inactive (Wu & Haber, 1996); therefore, the repair efficiency by 6 h is reduced compared to the H-1400 assay. We note that in all other assays tested here with *HMLα-inc* being the recombination template, RE is active. Interestingly, weak bands corresponding to both crossover products (< 5%) in wild-type cells were evident; such crossover products were not observed in recombination between *MATa* and *HMLα-inc*. Thus, the non-homologous Y sequence during *MAT* switching prevents lethal intrachromosomal crossovers in ~5% of the cells. Importantly in this assay, the BIR contribution increases in both *rad59Δ* and *rad52-R70A*, and viability decreases accordingly (Fig 2G–I). We noted above that BIR product has the same size as the larger of two crossover products. Considering that both crossover products form at the same time and the intensity of the shorter crossover product band is very weak or absent in annealing mutants, we conclude that BIR and not crossover is responsible for the increased intensity of this band in *rad59Δ* and *rad52-R70A* cells. In this assay, extended homology is present immediately on both sides of the break; thus, both ends could invade template early and prime BIR, one toward the telomere and one toward the centromere. However, BIR toward the centromere was not observed in the annealing mutants in this or any of the assays tested here with *HMLα-inc* serving as a template (Figs 2B and G, and EV3A). In all these assays, the Z-end invades and primes DNA synthesis toward the telomere. To test whether the centromere itself imposes a long-

range negative impact on BIR, we constructed an additional HR-0 recombination assay (Fig EV3B). In this assay, a DSB is induced at the *MAT $\alpha$*  locus. The Z-end of *MAT $\alpha$*  shares 230 bp homology with the *HMR $\alpha$ -inc* template, while the homology on the other end was eliminated entirely and the *HML* donor was deleted. Upon strand invasion, the Z-end primes DNA synthesis toward the centromere. Interestingly, only up to 3% of cells that induced the break synthesized a few kb of dsDNA in the direction of the centromere as measured 6 or even 10 h after DSB induction. Thus, BIR-specific

DNA synthesis is more efficient in the direction toward the telomere than the centromere. However, nearly complete lack of DNA synthesis in the direction of centromere is not related to the centromere itself, because the break at the *MAT* locus separates the chromosome fragment containing the invading Z-end and the template from the one carrying the centromere (Fig EV3B). Thus, some yet to be characterized chromatin or topological features may inhibit DNA synthesis at specific loci and orientation or, alternatively, proximity of telomeres have positive effect on BIR-specific DNA synthesis.

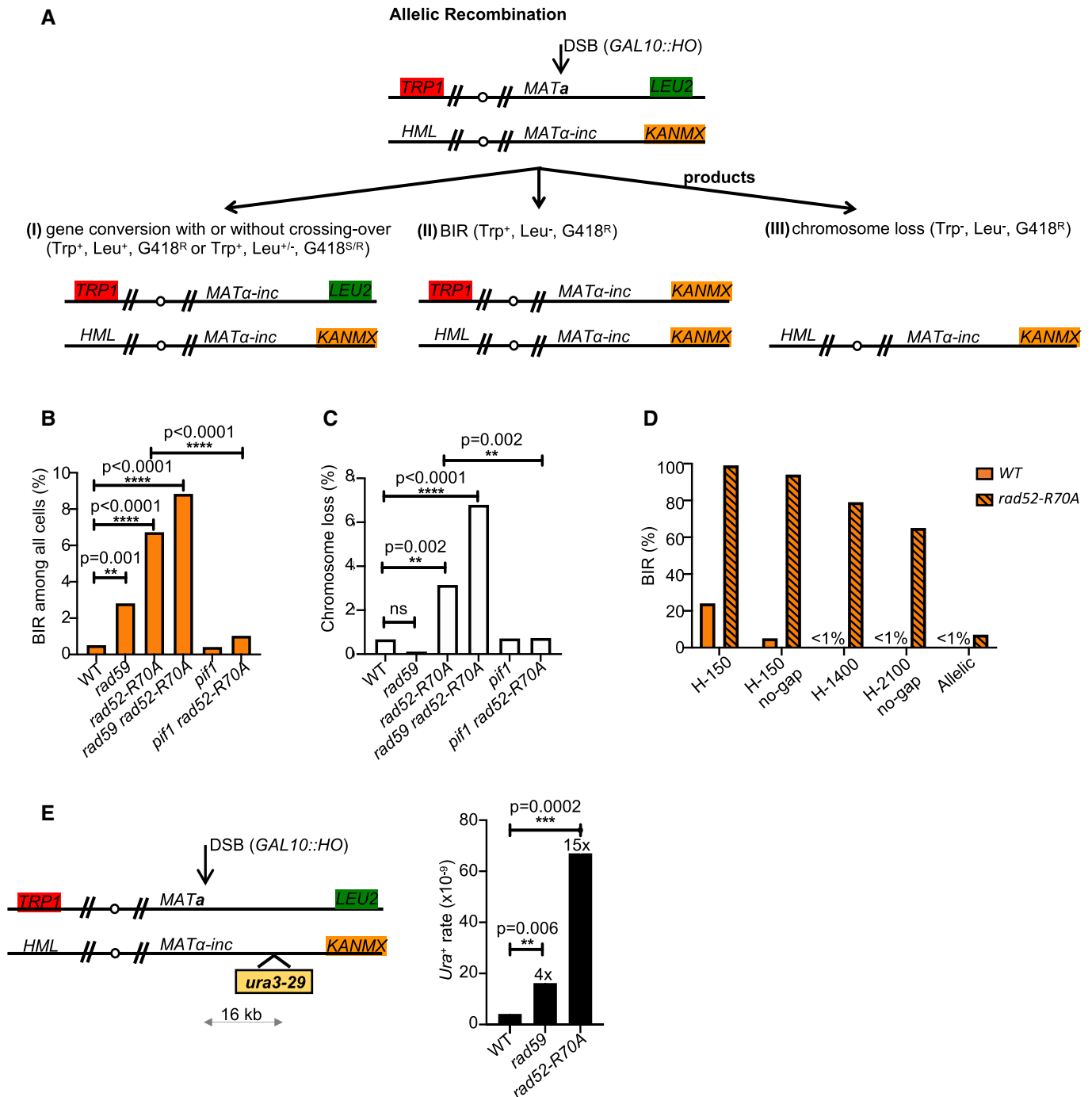


Figure 3.

**Figure 3. Longer homology mitigates the loss of Rad52 DNA binding domain and Rad59.**

- A Schematic of allelic recombination between two chromosomes III. A DSB is induced at *MAT $\alpha$*  and repaired by recombination with the homologous chromosome carrying *MAT $\alpha$ -inc*. Chromosome ends are marked with *TRP1*, *LEU2*, and *KANMX* to distinguish different repair products or chromosome loss. *Trp<sup>+</sup>*, *Leu<sup>-</sup>*, *G418<sup>R/S</sup>* colonies are scored as BIR products. Reciprocal sectored colonies (*Trp<sup>+</sup>*, *Leu<sup>-/+</sup>* *G418<sup>R/S</sup>*) represent gene conversion with crossover.
- B Percentage of BIR product among all cells are shown.
- C Percentage of chromosome loss of indicated mutants.
- D Comparison of BIR percentage among the products in different assays shown in Figs 1–3 in WT and *rad52-R70A* mutant cells. Percentage of repair products are measured at 6 h after break induction (H-150, H-1400, and H-2100 assays) or scored among plated cells (allelic assay) were pooled together.
- E Schematic of mutation analysis during allelic recombination (left). Mutation reporter cassette is inserted within the repair template 16 kb away from strand invasion site. Mutation rate (right) of WT, *rad59 $\Delta$* , *rad52-R70A* was calculated as previously described (Saini et al, 2013).

Data information: Chi-square test is used to determine the *P*-value in Fig 3B and C, number of colonies tested per mutant is indicated in Appendix Table S1. Mutation rates in Fig 3E are reported as the median value, and statistical comparisons between median mutation rates were performed using the Mann–Whitney *U* test. \**P*-value 0.01 to 0.05, significant; \*\**P*-value 0.001 to 0.01, very significant; \*\*\**P*-value 0.0001 to 0.001, extremely significant; \*\*\*\**P* < 0.0001, extremely significant; *P* ≥ 0.05, not significant (ns).

We also note that in the H-2100 or H-1400 assays, only 15–30% of *rad52-R70A* mutant cells repair the break by BIR, respectively (Fig 2E and J). This level of repair by BIR is far below the one observed in cells that lack any homology on the second end of a DSB (H-0, 60%). Thus, longer homology on the second end, particularly when it is located right next to the DSB end (H-2100), decreases BIR efficiency in annealing mutants. It is possible that with increased homology both DSB ends might simultaneously invade the template or Y-end invades first, which preclude BIR.

#### Increased homology partially alleviates the need for Rad52- and Rad59-mediated ssDNA annealing in recombination and in suppressing BIR

Using intrachromosomal *MAT* switching assays, we found that second end capture through ssDNA annealing stimulated by Rad59 and Rad52 is important to suppress the BIR pathway during the repair of two-ended DSBs. All of these assays have homology ranging from 150 bp to ~2 kb. Next, we tested whether Rad52 annealing activity restricts BIR in allelic recombination between two chromosomes III, where homology on each end is over 100 kb. To follow different products of DSB repair or chromosome loss in the allelic system, chromosome ends were marked with *TRP1*, *LEU2*, and *KANMX* (Fig 3A). *LEU2* and *KANMX* markers were inserted at subtelomeric regions of the right ends of the two chromosomes III. BIR products are viable and can be genetically distinguished from gene conversion with or without crossover and from chromosome loss (Fig 3A). In wild-type cells, fewer than 1% of cells repair the DSB by BIR. However, BIR increases ~6- to ~18-fold in *rad59 $\Delta$* , *rad52-R70A*, and *rad59 $\Delta$  rad52-R70A* mutant cells (Fig 3B, Appendix Table S1) while viability remains the same as in wild type (100%).

The helicase Pif1 is important for BIR as it facilitates D-loop migration (Wilson et al, 2013). As expected, elimination of Pif1 significantly reduced BIR in *rad52-R70A* mutant cells during allelic recombination (Fig 3B). Compared to *MAT* switching assays, we found that repair in the allelic system was far more efficient in all annealing mutants with only up to 7% chromosome loss (Fig 3C). With all assays taken together, it is clear that increased homology reduces the need for Rad52-mediated annealing for basic gene conversion (Fig 3D). It is possible that with longer homologous sequences, spontaneous Rad52-independent annealing is sufficient to complete DSB repair (Ozenberger & Roeder, 1991).

#### The increased BIR in annealing mutants is accompanied by an increase of mutations

BIR is an extremely mutagenic process owing to its specific mechanism limiting mismatch repair (Deem et al, 2011; Saini et al, 2013). To test whether increased BIR contribution to DSB repair between fully homologous chromosomes in annealing mutants is mutagenic, we inserted the *ura3-29* reporter gene 16 kb away from the break on the template chromosome and tested the level of mutations. We observed a 4- and 15-fold increase of mutation rate in *rad59 $\Delta$*  and *rad52-R70A* mutants, respectively, when compared to WT cells (Fig 3E). This result is consistent with the fact that the proportion of BIR among repair products increases in annealing mutants.

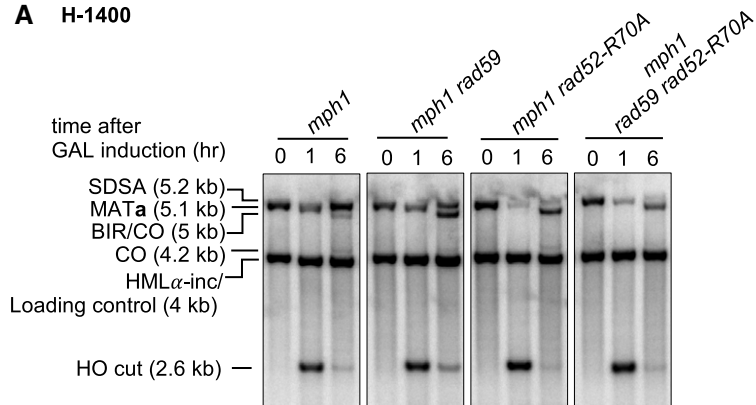
#### Role of Mph1 helicase in suppressing BIR at two-ended breaks

Mph1 is capable of unwinding D-loops formed during recombination and thus stimulates the SDSA pathway in budding and fission yeast (Sun et al, 2008; Prakash et al, 2009). Mph1 is also involved in D-loop unwinding during template switches in BIR (Stafa et al, 2014). Here, we constructed mutants defective in both D-loop unwinding and annealing, and tested BIR and SDSA contributions to the repair of two-ended breaks.

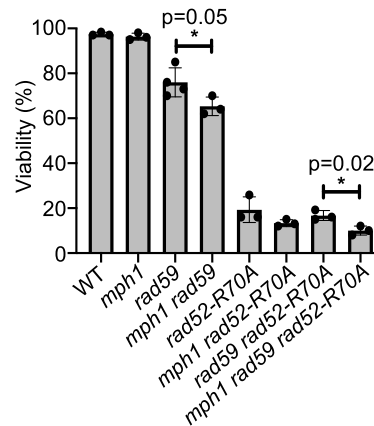
Previously it was demonstrated that elimination of Mph1 increases BIR in the repair of two-ended breaks when homology on the second end is short (Luke-Glaser & Luke, 2012; Mehta et al, 2017); however, this increase was much smaller than in annealing mutants. Here, we used recombination assays with longer homology to test the role of Mph1 in competition between SDSA and BIR. In regular mating-type switching where the second end carries 1.4 kb homology (H-1400 assay), crossovers are not visible among the products of *MAT* switching in wild-type cells (Fig 2B), while in *mph1 $\Delta$* , two weak crossover bands are observed. This result further supports the role of Mph1 in suppressing crossover outcomes (Fig 4A) (Prakash et al, 2009). The longer crossover band that also corresponds to the BIR product has a slightly stronger intensity than the shorter crossover band, suggesting that there is a very mild stimulation of BIR in *mph1 $\Delta$*  mutant cells. Accordingly, the viability of the *mph1 $\Delta$*  cells is comparable to the wild-type cells (Fig 4B and C). However, the elimination of Mph1 in annealing mutants, *rad59 $\Delta$*  or *rad52-R70A* further increased the BIR contribution to the repair, or nearly entirely switched repair to BIR (Fig 4A–D). In allelic recombination, the elimination of Mph1 by itself did not increase BIR events



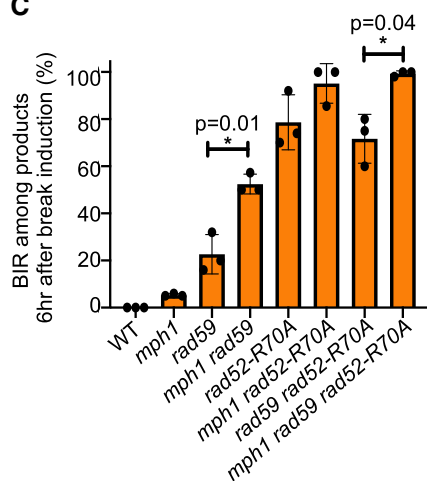
**A H-1400**



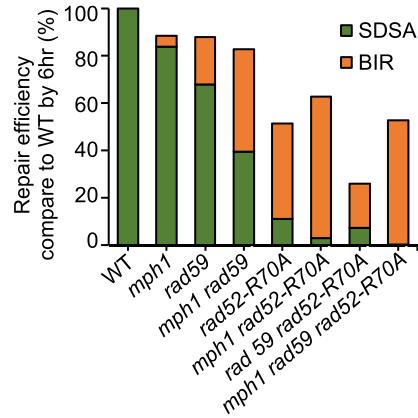
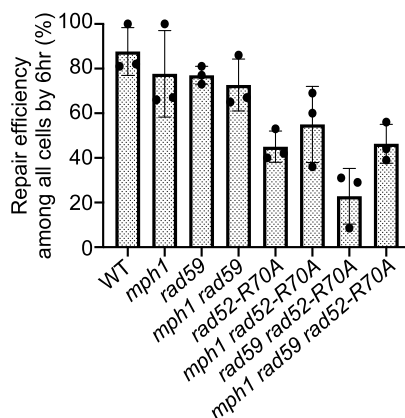
**B**



**C**



**D**



**E**

**Allelic Recombination**

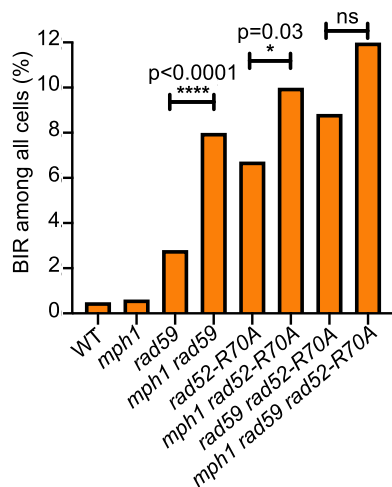


Figure 4.

**Figure 4. Role of Mph1 in suppressing BIR.**

Analysis of Mph1's role in regulating BIR outcomes in mating-type switching (A-D) or allelic recombination (E).

A Representative Southern blots showing DSB repair products of indicated mutants in regular mating-type switching (H-1400 assay).

B Viability of indicated mutants is shown. (Mean  $\pm$  SD;  $n = 3$ ).

C Percentage of BIR product among all repair products by 6 h are shown. (Mean  $\pm$  SD;  $n = 3$ ).

D Graphs show analysis of repair efficiency compared to uncut parental band (left) (mean  $\pm$  SD;  $n = 3$ ) and repair efficiency compared to WT (right) at 6 h after DSB induction (right). See Fig 1F for details.

E Percentage of BIR among all repair products in allelic recombination.

Data information: Welch's unpaired  $t$ -test was used to determine the  $P$ -value in Fig 4E. Number of colonies tested per mutant is indicated in Appendix Table S1. \* $P$ -value 0.01 to 0.05, significant; \*\* $P$ -value 0.001 to 0.01, very significant; \*\*\* $P$ -value 0.0001 to 0.001, extremely significant; \*\*\*\* $P < 0.0001$ , extremely significant;  $P \geq 0.05$ , not significant (ns).

at all. However, loss of Mph1 in annealing mutants increased the BIR level to  $\sim 12\%$  in triple *mph1 $\Delta$  rad59 $\Delta$  rad52-R70A* mutant cells (Fig 4E, Appendix Table S1). We conclude that with extensive homology, Mph1 by itself does not change BIR frequency; however, it suppresses BIR when ssDNA annealing activity is compromised.

**Sir2 suppresses BIR with a heterochromatic donor when homology is short**

The *HML* locus serves as a template for recombination in *MAT* switching in most of the assays described here (H-150, H-1400, H-2100). *HML* is heterochromatic and silenced by the Sir2 histone deacetylase (Weiss & Simpson, 1998). Highly positioned nucleosomes

could potentially affect the D-loop migration or D-loop unwinding and therefore impact BIR and SDSA choice. To determine whether the heterochromatic state of the recombination template affects the competition between BIR and SDSA, we constructed *sir2 $\Delta$*  derivatives of the H-150, H-150 no-gap, and H-1400 assays, in which the *HML* template is unsilenced. The presence of the *HML $\alpha$ -inc* allele prevents the cleavage of *HML* when it is unsilenced. In the H-150 assay, the contribution of BIR increased from  $\sim 20\%$  up to  $\sim 55\%$ , and the viability of *sir2 $\Delta$*  decreased accordingly, owing to the lethality of BIR events (Fig 5A). Similarly, BIR increased by twofold in the H-150 no-gap system (Fig 5B). We note that *sir2 $\Delta$*  cells in H-150 assay carrying *HML $\alpha$ -inc* and *MATa* express both mating-type genes. Previous studies have shown that cells expressing both *MATa1* and *HML $\alpha$ 2* genes

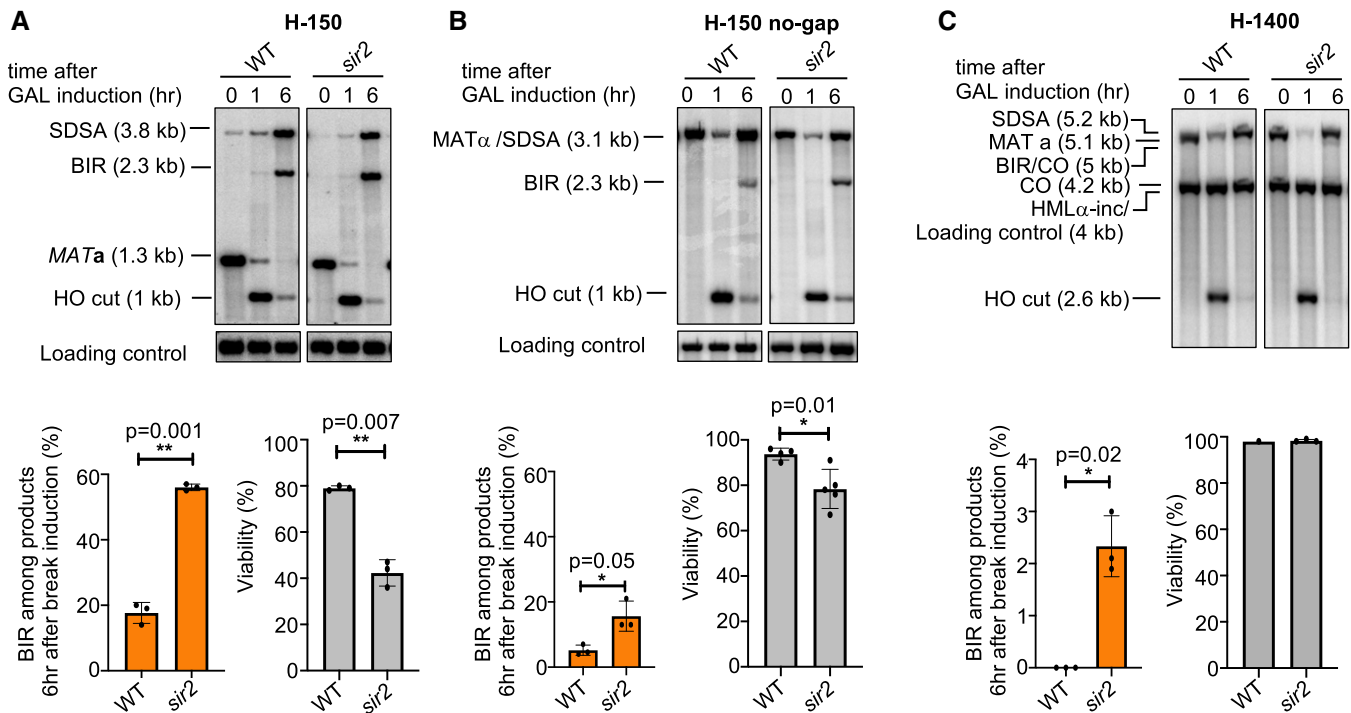


**Figure 5. Role of Sir2 in suppressing BIR during repair of two-ended breaks.**

A-C Representative Southern blots showing DSB repair products (top), percentage of BIR among repair products (bottom left), and viability (bottom right) of WT and *sir2 $\Delta$*  in the H-150 assay (A), H-150 no-gap assay (B), or native mating-type switching H-1400 assay (C). (Mean  $\pm$  SD;  $n = 3$ ). Welch's unpaired  $t$ -test was used to determine the  $P$ -value in panels A-C.

Data information: \* $P$ -value 0.01 to 0.05, significant; \*\* $P$ -value 0.001 to 0.01, very significant; \*\*\* $P$ -value 0.0001 to 0.001, extremely significant; \*\*\*\* $P < 0.0001$ , extremely significant;  $P \geq 0.05$ , not significant (ns).

exhibit some mating-type specific effects on DNA repair (Valencia-Burton *et al*, 2006). However, the effect of deleting *SIR2* on the competition between SDSA and BIR is not related to mating-type *per se*, as the increase of BIR was also observed in *sir2Δ* mutant cells in the system that expresses only  $\alpha$  genes (H-150 no-gap, Fig 5A and B). In

regular mating-type switching (H-1400 system), we also observe a minimal BIR increase in the *sir2Δ* mutant (~2%) and no change in viability (Fig 5C). We conclude that closed chromatin structure within the template has a role in suppressing BIR at DSBs, but mostly when homology at the second end is short.

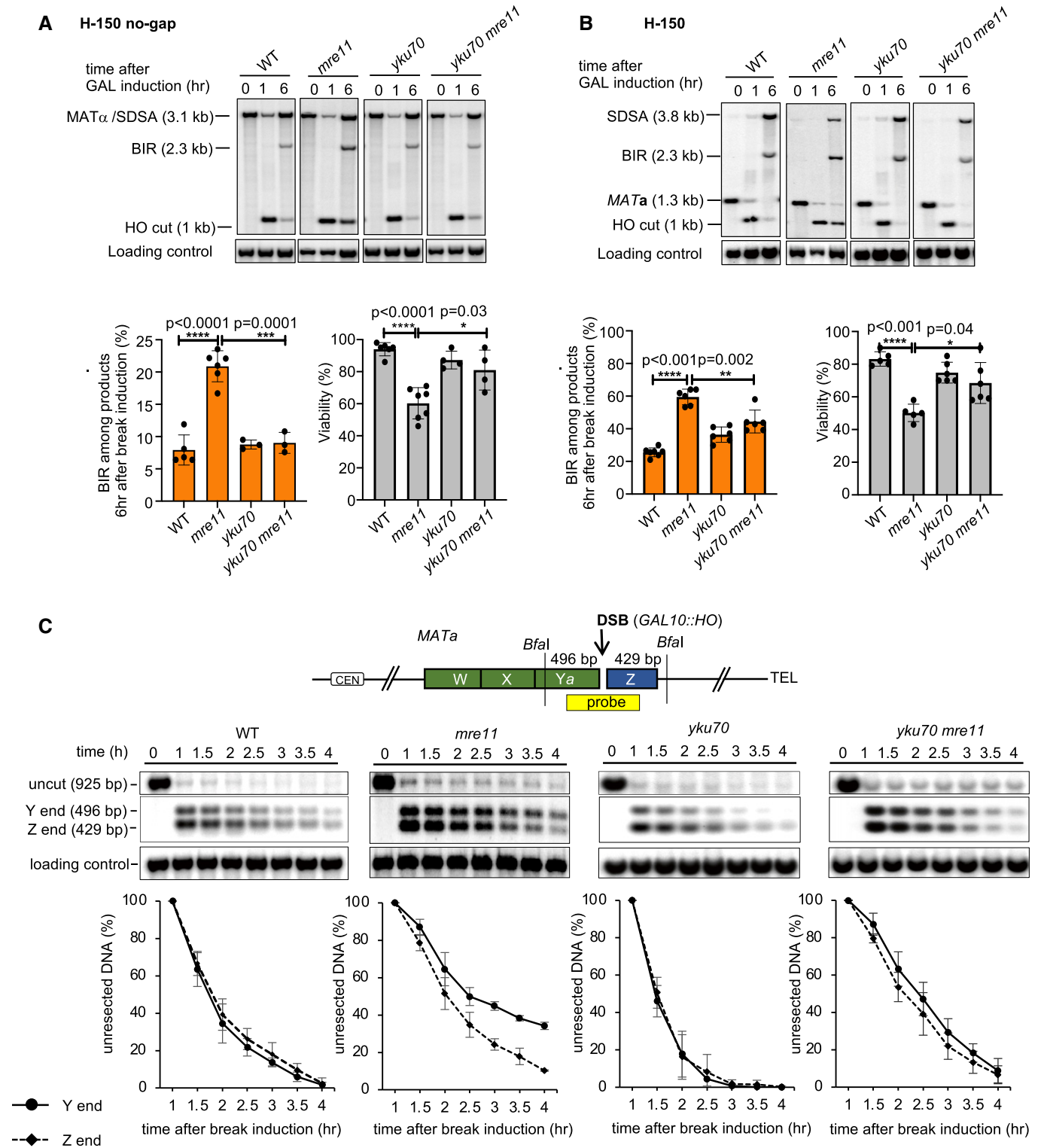


**Figure 6. Role of the MRX complex in suppressing BIR during repair of two-ended breaks.**

- A, B Representative Southern blots showing DSB repair products (top), percentage of BIR among repair products (bottom left), and viability (bottom right) of indicated mutants in the H-150 no-gap assay (A) or H-150 assay (B). (Mean  $\pm$  SD;  $n \geq 3$ ). Welch's unpaired t-test was used to determine the *P*-value in panels A and B.
- C Schematic of resection assay with sites of restriction enzyme *Bfal* cleavage and location of probe (top), representative of Southern blots, and graph showing kinetics of resection two break end (bottom) (mean  $\pm$  SD;  $n = 3$ ) in WT, *mre11Δ*, *yku70Δ*, and *yku70Δ mre11Δ*.

Data information: \**P*-value 0.01 to 0.05, significant; \*\**P*-value 0.001 to 0.01, very significant; \*\*\**P*-value 0.0001 to 0.001, extremely significant; \*\*\*\**P* < 0.0001, extremely significant; *P*  $\geq$  0.05, not significant (ns).

Source data are available online for this figure.

In these three assays, the *HML* template is within silent chromatin and *SIR2* deletion leads to unsilencing of the *HML* template. Next, we used an established assay in which the template is within the unsilenced region of the genome and the deletion of *SIR2* should have no impact on the chromatin state of the template. An HO-induced DSB at the *URA3* gene on chromosome V is repaired with a partial *URA3* region inserted on the opposite arm of the chromosome (Anand *et al*, 2014). The homology on each side of the break ("R" and "A" end) is 300 bp (Fig EV4A). In wild-type cells, only 0.8% of the cells repair the break by BIR (Anand *et al*, 2014). While we observed an over 30-fold increase of BIR in *rad52-R70A* annealing mutant cells, we did not see any change in BIR frequency in *sir2Δ* cells in this system, suggesting that the role of Sir2 in BIR regulation is related to the chromatin state of the template (Fig EV4B). A closed chromatin structure within the template could promote SDSA by slowing down the D-loop migration and/or making the D-loop more prone to unwinding. We favor the second possibility as the kinetics of BIR in *sir2Δ* cells, tested in H-0 system, are only modestly increased when compared to wild-type cells (Fig EV4C).

**The MRX complex suppresses BIR at two-ended DSBs**

The MRX complex plays an important role in the initial DSB end resection (reviewed in (Symington, 2016)) and in DSB ends tethering (Kaye *et al*, 2004; Lobachev *et al*, 2004; Jain *et al*, 2016a). To test the role of the MRX complex in regulation of BIR during the repair of two-ended DSBs, we used the H-150 and H-150 no-gap assays. In *mre11Δ* mutant cells, we observed about 2- to 3-fold increase of BIR in both assays (Fig 6A and B). Even when homology on the second end of the break is extensive in the allelic recombination assay, BIR still increased modestly in *mre11Δ/mre11Δ* (Fig EV5A). Colonies that showed a marker pattern typical for BIR products (Leu<sup>-</sup>, Trp<sup>+</sup>, and G418<sup>R</sup>) were further evaluated by CHEF and Southern blot to make sure that these are products of expected BIR size. 19 of 21 colonies tested by CHEF carried the expected BIR product size (Fig EV5B) while the remaining two colonies corresponded to chromosomal rearrangements. We conclude that MRX suppresses BIR events during repair of two-ended DSBs.

**Mre11 promotes synchronous resection of two DSB ends**

The MRX complex could coordinate both DSB ends in repair and suppress BIR by tethering two DSB ends or by promoting the synchronous resection of two DSB ends. It was previously suggested that MRX plays a role in synchronous resection of DSB ends (Westmoreland *et al*, 2009; Westmoreland & Resnick, 2013). Here, we tested whether HO-induced DSB ends at the *MAT* locus were synchronously resected in wild-type and in *mre11Δ* mutant cells.

The initial resection was monitored every 30 min up to 4 h after DSB induction using Southern blots and a probe specific for the *MAT* locus (Fig 6C). We note that in a population of cells, the asynchrony of resection can be observed only if the average resection kinetics of the centromere proximal DSB end (Y-end) and telomere proximal DSB end (Z-end) are different. Since resection cannot be monitored in individual cells using this method, stochastic asynchrony at two break ends could not be detected. As shown in Fig 6C, both ends of the break are resected with equal kinetics in wild-type cells, while in *mre11Δ* cells the resection of the Y-end is slower. In ~15–25% of *mre11Δ* cells, where the Z-end remained unresected by 3–4 h, we cannot test whether the Y-end was resected. Therefore, while Z-end is resected faster overall, we could not exclude the possibility that the Y-end is resected faster in some cells. Asynchrony of resection observed in *mre11Δ* cells may explain the increase of BIR observed at two-ended DSBs.

The resection defect of MRX mutants can be partially suppressed by the elimination of the Ku complex (Lee *et al*, 1998; Mimitou & Symington, 2010; Shim *et al*, 2010). Consistent with previous publications, the deletion of the *YKU70* increased resection kinetics, and this increase was observed on both ends of the break (Fig 6C). Also, *yku70Δ* partially suppressed the defect of resection in *mre11Δ* cells on the Y-end, but surprisingly it had nearly no effect on the Z-end where resection remained as slow as in *mre11Δ* single mutant cells (Fig 6C). This result suggests that the Ku complex by itself or in combination with other proteins forms a stronger barrier for MRX-independent resection on the Y-end. In *mre11Δ* cells in both the H-150 and H-150 no-gap assays, the deletion of *YKU70* lead to a significant decrease of BIR. This result suggests that the synchronous resection of two DSB ends is important to reduce BIR events. Altogether, the role of MRX in suppressing BIR at two-ended breaks is related to synchronous resection rather than tethering of two ends of the break. However, it is possible that these two functions may be related to each other. We note that expression of *MRE11-NLS* in *xrs2Δ* mutant strain restores ends resection and DSB repair by SDSA but not ends tethering. This result provides further support for the role of resection rather than end tethering in proper DSB repair (Oh *et al*, 2018).

**Discussion**

DNA breaks can be repaired by many different pathways of recombination, some of which are mutagenic and normally suppressed. BIR is one of the pathways that drives genome instability as it results in mutations, nonreciprocal translocations, and loss of heterozygosity (reviewed by (Sakofsky & Malkova, 2017)). Here, we aimed to understand the mechanism that limits the use of BIR in the

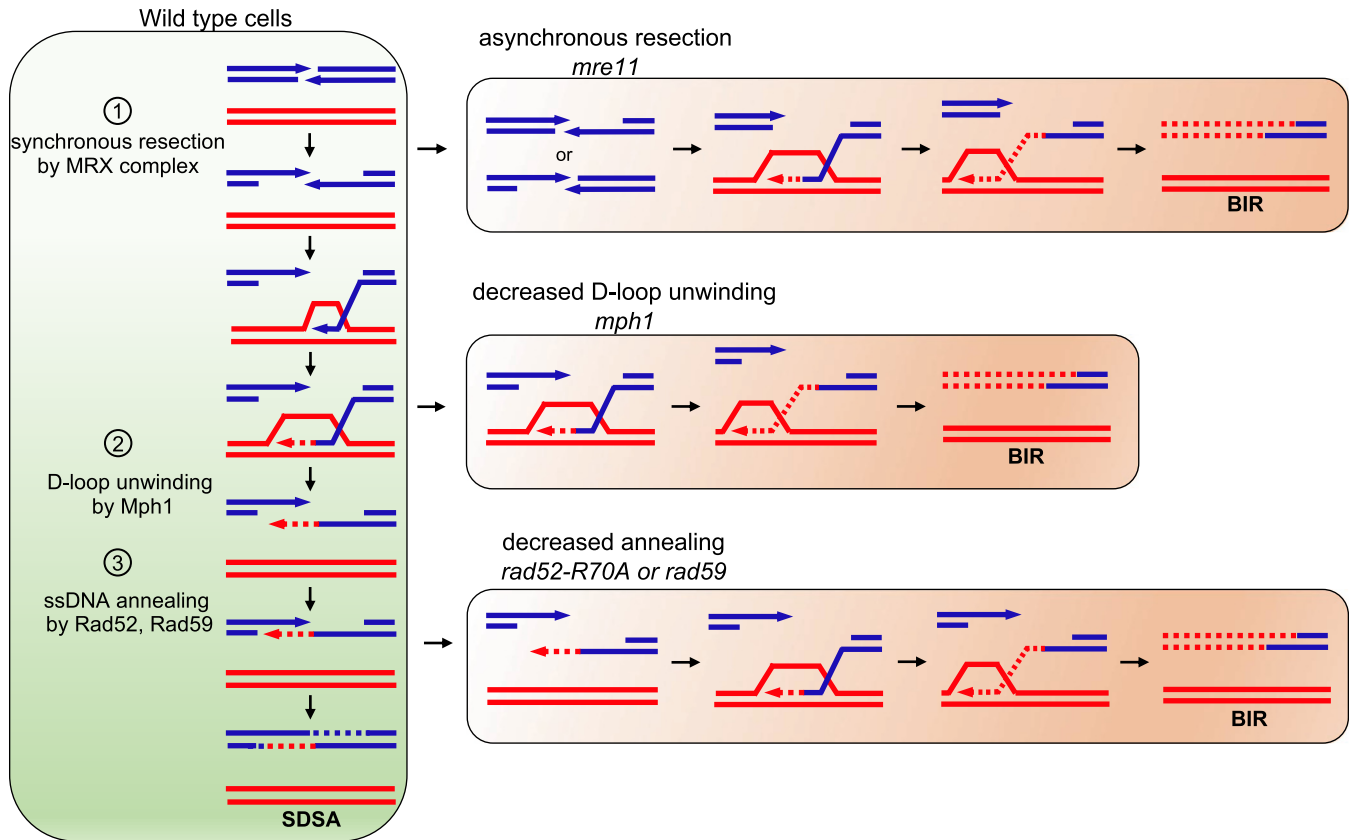


**Figure 7. Model presenting multiple mechanisms restraining Break-Induced Replication at two-ended DNA double-strand breaks.**

Several proteins coordinating the usage of two ends of a DSB suppress BIR: (1) Mre11-Rad50-Xrs2 complex (MRX) that promotes synchronous resection of two ends of a DSB, (2) D-loop unwinding helicase Mph1 that stimulates SDSA, and (3) ssDNA annealing proteins Rad52 and Rad59 that promote second end capture. All of these proteins are particularly important to reduce BIR when recombination occurs between short repetitive sequences.

repair of two-ended breaks. We identified several independent mechanisms that impair BIR, as shown in Fig 7. Two-ended breaks are usually repaired by the SDSA mechanism in growing cells, resulting in a short-patch DNA synthesis by polymerase  $\delta$  (Ira *et al*, 2006; Maloisel *et al*, 2008; Guo *et al*, 2017). An essential step in the repair is to engage both ends of a DSB, thus eliminating the possibility that the invading end primes excessive DNA synthesis up to the end of the chromosome via BIR. We hypothesized that by eliminating activities that coordinate the usage of two ends of a DSB in SDSA, the contribution of BIR would increase. We found that the loss of ssDNA annealing activity in *rad52-R70A* or *rad59 $\Delta$*  increases BIR at two-ended breaks. We propose that compromised ssDNA annealing prevents the second end from annealing to the extended and displaced 3' strand in the SDSA mechanism, or from capturing the extended D-loop in a double Holliday junction mechanism. In these scenarios, BIR synthesis via a migrating D-loop can reach the end of the chromosome. However, decreased annealing has a milder effect on overall repair by gene conversion and BIR when homology at the second end is extensive. This result leads to an intriguing question: How are two-ended breaks repaired in mutants severely deficient in ssDNA annealing? It is possible that spontaneous annealing is sufficient for gene conversion when homology is long, as proposed previously in SSA (Ozenberger & Roeder, 1991).

Alternatively, with extended homology on both sides of the DSB, both ends could invade the template and be resolved as a gene conversion, thus reducing the chance that the D-loop migrates to the end of the chromosome. Finally, we cannot exclude the possibility that there is an additional protein capable of weak ssDNA annealing during recombination, such as Mcm10 (Mayle *et al*, 2019). Notably in fission yeast, Rad52 annealing activity seems to be mostly dispensable for DSB repair, as *rad52 $\Delta$*  cells are resistant to DNA damage so long as cells are capable of loading Rad51 in a Rad52-independent manner (Osman *et al*, 2005).

DNA helicases also coordinate the use of two ends of a DSB. Mph1 unwinds the extended 3' strand that subsequently anneals with the second DSB end during SDSA. A more stable D-loop in the *mph1 $\Delta$*  mutant cells likely results in increased D-loop migration and BIR as previously proposed (Luke-Glaser & Luke, 2012; Mehta *et al*, 2017). Furthermore, *mph1 $\Delta$*  cells increase BIR when gene conversion is not in competition (Jain *et al*, 2016b), presumably by preventing unwinding of the initial strand invasion intermediate. BIR suppression by Mph1 in competition with gene conversion is particularly strong with shorter homologous sequences at the second DSB end. It is likely that besides Mph1, other DNA helicases also coordinate the use of two DSB ends. Yeast Srs2 is capable of unwinding D-loops, particularly when they are longer (Liu *et al*,

2017). Consequently, the elimination of Srs2 leads to an increase of crossover products (Ira *et al.*, 2003; Robert *et al.*, 2006; Mitchel *et al.*, 2013). Thus, besides Mph1, Srs2 may also suppress BIR. However, we have not tested Srs2 here because Srs2 itself is very important for BIR (Elango *et al.*, 2017).

The effect of mutating enzymes regulating BIR frequency is partially (e.g., annealing mutants) or entirely (e.g., *mph1Δ*) mitigated by increased homology. This observation suggests that the control of BIR at two-ended breaks by enzymes coordinating the engagement of two DSB ends is essential in recombination between short repeated sequences and, thus, in genomes carrying many repetitive elements, such as human genome. Longer homology on the second end of the break likely increases the chance of the initiation of recombination by second end of the DSB. Recently, we have shown that head-on collisions by transcription prevent BIR and it is likely that assembling the repair apparatus on the opposite end may also inhibit BIR (Liu *et al.*, 2021).

Another protein complex that may coordinate the use of two ends of a DSB is the MRX complex. Mutants deficient in MRX show frequent (10–20%) separation of two ends of a DSB (Kaye *et al.*, 2004; Lobachev *et al.*, 2004; Jain *et al.*, 2016a). This result suggests that MRX is important for holding two DSB ends together. The MRX complex also coordinates the resection at ionizing radiation-induced DSB ends (Westmoreland *et al.*, 2009; Westmoreland & Resnick, 2013), and the synchronous resection of two ends is likely important to engage them in HR at the same time. Indeed, we found that in the absence of Mre11, repair of two-ended DSBs by BIR increases. Careful analysis of resection showed that two ends of the break are not processed synchronously in *mre11Δ* cells. In a population of cells, the telomere proximal end of the break is processed faster. Deletion of *YKU70* in *mre11Δ* cells restores synchronous resection of the two ends and decreases the BIR level among the products. Thus, we conclude that the Ku complex by itself or in combination with other proteins or specific DNA sequences forms a barrier for MRX-independent resection more efficiently on one of two DSB ends. This barrier results in asynchronous formation of ssDNA and increase of BIR. We note that we cannot exclude the possibility that tethering of DSB ends by MRX also contributes to regulation of SDSA/BIR as synchronous resection of two ends may require ends tethering.

Mating-type switching normally occurs between the HO-cleaved euchromatic *MAT* locus and the heterochromatic donor *HML*. We found that Sir2's maintenance of this heterochromatic state is important for suppressing BIR, particularly when homology is short. It is possible that histone deacetylation and the highly ordered nucleosomes within *HML*'s chromatin structure interfere with D-loop migration, thus resulting in easier D-loop disruption. Polδ, which is responsible for lagging strand synthesis during replication, usually stops DNA synthesis at the point where the interaction between DNA and histones is strongest (Smith & Whitehouse, 2012). Thus it is possible that Polδ-mediated DNA synthesis in BIR is less effective within dense chromatin. We note also that BIR is a pathway used to extend telomeres in telomerase deficient cells (review in (Lee *et al.*, 2020)), and telomeres reside within heterochromatin. However, telomere silencing is weaker when compared to *HML* silencing (review in Haber, 2012), so BIR through telomeric regions might be easier than through the *HML* locus. Alternatively, the chromatin state at subtelomeric regions could change during telomere length crisis.

Together this work determines the function of many recombination enzymes in suppressing one of the most mutagenic DSB repair pathways, BIR. Rad52 is highly conserved, but in many eukaryotes it plays a less prominent role in HR. In these organisms, additional annealing enzymes evolved with a role in HR such as FANCA in humans, the annealing helicase SMARCAL1 in flies, or Bhr2, the BRCA2 homolog in *U. maydis* (Mazloum & Holloman, 2009; Holsclaw & Sekelsky, 2017; Benitez *et al.*, 2018). The MRX complex and D-loop unwinding enzymes are also well conserved between yeast and humans. These enzymes likely prevent mutagenic BIR in higher eukaryotes in a similar way as observed in yeast, particularly when recombination occurs between short homologous repeats.

This work also shows that BIR is not efficient everywhere in the genome. Even in the same *HML* locus, BIR is efficient in the direction of the telomere and inefficient or absent in the direction of the centromere, but is apparently not dependent on the centromere itself. Favoring BIR toward telomere over centromere has implications for genome stability. Since telomeric distal regions are devoid of essential genes, the outcome of mutagenic BIR toward telomere is more tolerable. BIR toward the telomere could also be beneficial evolutionarily, as the duplication and exchange of genetic material in subtelomeric regions could increase the diversity of subtelomeric gene families (Brown *et al.*, 2010). Chromosomal features determining BIR efficiency at specific loci or direction remain unknown. It remains to be determined whether some local topology, cohesion, or other chromosome features interfere with extensive D-loop migration required for BIR.

## Materials and Methods

### Strains and plasmids

All strains used in this study are presented in Appendix Table S2.

To study competition between SDSA and BIR using intrachromosomal recombination, we used YAM033 and its derivatives listed in Appendix Table S2 (*ho ade3::GAL10::HO HMLα-inc MATa hmr::ADE1 bar1::ADE3 nej1::KANMX ade1 leu2,3-112 trp1::hisG ura3-52 thr4 lys5*) (Mehta *et al.*, 2017). To construct strains with different homology size on one end of the DSB at *MAT*, complete/partial deletions of W, X, Yα were made by integrating *Candida glabrata* *TRP1*, amplified out from YAM033, (primers listed in Appendix Table S3). To make the H-150 assay, complete deletion of W, and partial deletion of X within *MATa*, leaving 150 bp, was constructed as described (Mehta *et al.*, 2017). To make the “H-150 no-gap” assay, we created a complete deletion of W, X, and most of the Yα sequence within *MATα*, leaving just 150 bp of Yα. For the H-0 assay, all W and X sequences were completely deleted in *MATa*. The H-1400 assay represents regular *MAT* switching between *MATa* and *HMLα-inc*, while the H-2100 assay represents recombination between *MATα* and *HMLα-inc*.

Another recombination on chromosome V system was further used to test the competition between SDSA and BIR. The strain yRA97 was gifted from Haber lab (*hoΔ mat::hisG hmlΔ::hisG HMRA-stk ura3Δ851 trp1Δ63 leu2Δ::KAN hmrΔ::ADE3 ade3::GAL10::HO can1Δ::UR::HOcs::A3::TRP1 RA::LEU2*) (Anand *et al.*, 2014).

To study the outcomes of the allelic recombination, we used derivatives of JKM139 (*ho hml::ADE1 MATa hmr::ADE1 ade1 leu2-*

3,112 *lys5 trp1::hisG ura3-52 ade3::GAL10::HO*) and NP633 (*MAT $\alpha$ -inc HML $\alpha$ -inc hmr::ADE1 bar1::ADE3 ade1 leu2,3-112 trp1::hisG ura3-52 thr4 lys5 ade3::GAL10::HO*). To mark the ends of chromosome III in JKM139, a *kiTRP1* marker was inserted at location 17130, and a *LEU2* marker was inserted at position 296670 to create strain NP676, and in NP633 the *KANMX* marker was inserted at position 296670 to generate strain NP643. DNA repair genes listed in Appendix Table S2 were deleted in NP676 and NP643, and resulting haploid mutant strains were crossed to obtain diploids for allelic recombination analysis.

To estimate the mutation rate ~16 kb away from the DSB end during allelic recombination, we first eliminated *ura3-52* from strains NP676 and NP643 using CRISPR/Cas9 methods to construct NP729 and NP728 respectively. Plasmid NP633 was made by cloning gRNA targeting *URA3* (sequence listed in Appendix Table S3) into plasmid bRA89 after digestion with *BpI* as published (Anand et al, 2017). The deletion of *ura3-52* was obtained by transforming cells with plasmid NP633 and *URA3* deletion template DNA. The deletion was confirmed by PCR and Sanger sequencing. The *ura3-29-HPH* fragment was generated by PCR amplification using primers listed in Appendix Table S3 and inserted ~16 kb distal to *MAT $\alpha$ -inc* in the donor parent strain NP728, resulting in strain NP754. The *ura3-29* mutation reporter (Shcherbakova & Pavlov, 1996) can revert to *Ura*<sup>+</sup> via three different base substitutions at one C-G pair. Haploid strains NP729 and NP754 were crossed to obtain diploid NP757, and mutation rates were estimated as previously described (Saini et al, 2013). Diploid strains lacking DNA repair enzymes were constructed for mutation rate analysis as described above and are presented in Appendix Table S2.

Strains carrying BIR assay between two chromosomes III are derivatives of strain AM1003 (*MAT $\alpha$ -LEU2-tel/MAT $\alpha$ -inc ade1 met13 ura3 leu2-3,112/leu2 thr4 lys5 hml::ADE1/hml::ADE3 hmr::HYG ade3::GAL-HO FS2::NAT/FS2*) (Deem et al, 2008).

Strain to study DNA synthesis during BIR toward the centromere (HR-0) was constructed by deleting all W and X sequences at *MAT $\alpha$* . A DSB is induced at *MAT* locus, invasion at Z sequence of *HMR $\alpha$ -inc* template leads to repair by BIR.

Mutagenesis of arginine 70 to alanine (R70A) in *RAD52* to make DNA binding-defective *rad52-R70A* mutant was done using CRISPR-Cas9 methods. We note that *RAD52* contains multiple putative start codons (Mortensen et al, 2002). In this work, *RAD52* sequence starts from the first start codon and the annealing mutants correspond to R70A. In modified and shorter by 33 residues *RAD52* gene in SGD database, it begins at the third ATG and annealing mutant corresponds to R37A. gRNA targeting *RAD52* was cloned into plasmid bRA90 to construct plasmid NP511. Cells were then transformed with NP511 and *rad52-R70A* template DNA to construct the *rad52-R70A* mutant. Mutation was then confirmed by Sanger sequencing.

### Viability assays

To determine the viability, cells were grown overnight in YEP-raffinose medium (1% yeast extract, 2% peptone, 2% raffinose), and ~100 cells were plated onto YEPD and YEP-galactose plates. Colonies were counted 3–5 days after plating. The proportion of viable cells was estimated by dividing the number of colony-forming units on YEP-galactose plates by that on YEPD plates. Statistical

comparison between mutants was performed using Welch's unpaired *t*-test and Prism 8 software.

### Growth and induction of DSB in yeast

Yeast cells were grown overnight in YEPD (1% yeast extract, 2% peptone, 2% dextrose) and transferred to YEP-raffinose medium (1% yeast extract, 2% peptone, 2% raffinose) for ~16 h. HO was induced when the cell density was  $\sim 1 \times 10^7$  cells/ml by adding galactose to a final concentration of 2%. Samples were collected for DNA isolation just before and at different time points following the addition of galactose.

### Analysis of BIR and SDSA by Southern blot

DNA was isolated by glass bead disruption using a standard phenol extraction protocol. DNA was digested with either *Bsp1286I* (H-0 and H-150, H-150 no-gap system) or *EcoRI* and *XhoI* (H-1400 and H-2100 system) and separated on 0.8% agarose gels. Southern blotting and hybridization with radiolabeled DNA probes were carried out as described previously (Church & Gilbert, 1984). Southern blots were probed with a <sup>32</sup>P-labeled *MAT $\alpha$ -distal* or Z fragment. All primers used to amplify the probes are listed in Appendix Table S3. All quantitative densitometric analysis was done using ImageQuant TL 5.2 software (GE Healthcare Life Sciences). To control for differences in the amount of DNA loaded into each lane, each fragment of interest was normalized to a loading control fragment: *ACT1* fragment (H-0, H-150, and H-150 no-gap) or Z fragment of *HML $\alpha$ -inc* H-1400 and H-2100 system). Percentage of BIR among the products measured at 6 h after DSB induction was calculated as the percentage of the pixel intensity of the band corresponding to BIR to the total pixel intensity of the bands corresponding to both BIR and SDSA products. In rare cases, a very weak crossover band was observed. In these cases, the intensity of the shorter crossover band was subtracted from the band that corresponds to both the longer crossover band and BIR. Repair efficiency among all cells of each mutant was calculated as the percentage of normalized pixel intensity of bands corresponding to both BIR and SDSA products at 6 h to the normalized pixel intensity of the parental band at 0 h. Repair efficiency compared to WT was measured as the percentage of normalized pixel intensity of bands corresponding to either BIR or SDSA at 6 h of a mutant to the normalized pixel intensity of bands corresponding to BIR and SDSA at 6 h of WT cells. Statistical comparison of the percentage of BIR and repair efficiency between different mutants was performed using Welch's unpaired *t*-test (Prism 8 software).

### Analysis of allelic recombination assay

Allelic recombination between chromosomes III was analyzed using diploid strains where each parental haploid strain carried chromosome III with different markers to follow different repair products, as described in Fig 3. The assay was performed by growing cells overnight in YEP- raffinose medium, and ~50–70 cells were plated onto YEPD and YEP-galactose plates. After 3–5 days, replica plating on tryptophan dropout, leucine dropout, or YEPD plates supplemented with G418 to score different repair outcomes. BIR is scored as *Trp*<sup>+</sup>, *Leu*<sup>-</sup>, *G418R*, chromosome loss is scored as *Trp*<sup>-</sup>, *Leu*<sup>-</sup>,

*G418R*. Gene conversion without crossing-over is scored as *Trp*<sup>+</sup>, *Leu*<sup>+</sup>, *G418R*. Gene conversion with crossover will generate *Trp*<sup>+</sup>, *Leu*<sup>-</sup>, *G418R/Trp*<sup>+</sup>, *Leu*<sup>+</sup>, *G418S* sectored colonies, and *Trp*<sup>+</sup>, *Leu*<sup>+</sup>, *G418R* colonies. Since gene conversion without crossover is also scored as *Trp*<sup>+</sup>, *Leu*<sup>+</sup>, *G418R* colonies, the counted number of *Trp*<sup>+</sup>, *Leu*<sup>-</sup>, *G418R/Trp*<sup>+</sup>, *Leu*<sup>+</sup>, *G418S* sectored colonies is then doubled to reflex the actual number of gene conversion with crossover and the number of gene conversion without crossover will be then subtracted accordingly.  $\chi^2$  analysis was used to perform a statistical comparison between mutants for individual classes of events using Prism 8 software.

### Mutation analysis

To determine mutation frequency associated with BIR, cells were grown overnight in YEPD, followed by growth in YEP-raffinose to the concentration of  $\sim 1 \times 10^7$  cells/ml. Breaks were induced by adding galactose to a final concentration of 2%, and cells were incubated for 6 h.  $\sim 3\text{--}5 \times 10^8$  cells were plated on uracil dropout plate (s) before (0 h) and 6 h after galactose addition. The number of colonies was counted after 3–5 days. The mutant frequency was calculated as  $f = m/N$  ( $m$  is the total number of mutants in a culture, and  $N$  is the total number of cells in a culture). Since the experimental strains did not divide or underwent a single division between 0 h and 6 h, the rate of mutations after galactose treatment was determined using a simplified version of the Drake equation:  $\mu_6 = (\phi_6 - f_0)$ , where  $f_6$  and  $f_0$  are the *Ura*<sup>+</sup> mutation frequencies at times 6 h and 0 h, respectively. Rates are reported as the median value, and statistical comparisons between median mutation rates were performed using the Mann–Whitney *U* test as previously described (Saini et al, 2013).

### CHEF analysis of allelic recombination products

To analyze BIR repair products scored by plating assay, chromosomal DNA plugs were prepared and separated on 1% agarose gel at 6 V/cm for 48 h (initial time = 20 s, final time = 30 s) by using the CHEF DRII apparatus (Bio-Rad), followed by Southern blotting and hybridization with a *TRP1* sequence as a probe.

### Analysis of allelic BIR

BIR assay using a disomic strain with an extra, truncated copy of chromosome III was previously described (Saini et al, 2013). The BIR assay was performed by growing cells overnight in 2% raffinose medium, and  $\sim 100$  cells were plated on YEP-galactose plates to induce the break and on YEPD as control. Different repair outcomes were score after 3–5 days by replica plating on adenine dropout, YEPD plates supplemented with *G418*, or clonNAT to score different repair outcomes.

### Analysis of recombination assay on chromosome V

A same number of cells were plated on YEPD to get the total cell count and on YEP-galactose plates for HO induction. Cells that grew on YEP-galactose were counted and replica-plated to replica plating on uracil, tryptophan, or leucine dropout plates to screen for different repair outcomes.

### Resection analysis

Resection analysis was done as previously described (Zhu et al, 2008). Cells were cultured overnight in raffinose to the concentration of  $1 \times 10^7$ /ml. Cells were collected at 0 h before galactose was added to the culture to the final concentration of 2% to induce the break. Cells were then collected every 30 min (Fig 6) or every 2 h (Appendix Fig S2). DNA isolated by glass bead disruption using a standard phenol extraction protocol was digested with BfaI or EcoRI. Southern blot and hybridization with radiolabeled DNA MAT and loading control BPL1 were used to monitor 5' strand resection beyond the BfaI or EcoRI site. All quantitative densitometric analysis was done using ImageQuant TL 5.2 software (GE Healthcare Life Sciences).

### Data availability

This study includes no data deposited in external repositories.

**Expanded View** for this article is available online.

### Acknowledgements

We thank members of the Ira laboratory for critical reading of the manuscript. This work was funded by grants from the National Institute of Health (GM080600 and GM125650 to G.I., R35 GM127029 to J.E.H., R35GM127006 to A.M.).

### Author contributions

NP constructed strains, designed, conducted, and analyzed data. ZY helped with construction of Rad52 point mutant, YY helped with resection analysis, and MFA helped with analysis of repair events in yRA97 strain. NP, AM, and JEH and GI designed experiments, analyzed the data, and wrote the manuscript.

### Conflict of interest

The authors declare that they have no conflict of interest.

### References

- Anand R, Beach A, Li K, Haber J (2017) Rad51-mediated double-strand break repair and mismatch correction of divergent substrates. *Nature* 544: 377–380
- Anand RP, Tsaponina O, Greenwell PW, Lee CS, Du W, Petes TD, Haber JE (2014) Chromosome rearrangements via template switching between diverged repeated sequences. *Genes Dev* 28: 2394–2406
- Bai Y, Davis AP, Symington LS (1999) A novel allele of RAD52 that causes severe DNA repair and recombination deficiencies only in the absence of RAD51 or RAD59. *Genetics* 153: 1117–1130
- Beck CR, Carvalho CMB, Akdemir ZC, Sedlazeck FJ, Song X, Meng Q, Hu J, Doddapaneni H, Chong Z, Chen ES et al (2019) Megabase length hypermutation accompanies human structural variation at 17p11.2. *Cell* 176: 1310–1324 e1310
- Benitez A, Liu W, Palovcak A, Wang G, Moon J, An K, Kim A, Zheng K, Zhang Y, Bai F et al (2018) FANCA promotes DNA double-strand break repair by catalyzing single-strand annealing and strand exchange. *Mol Cell* 71: 621–628.e4



- Bhowmick R, Minocherhomji S, Hickson ID (2016) RAD52 facilitates mitotic DNA synthesis following replication stress. *Mol Cell* 64: 1117–1126
- Brown CA, Murray AW, Verstrepen KJ (2010) Rapid expansion and functional divergence of subtelomeric gene families in yeasts. *Curr Biol* 20: 895–903
- Carvalho CM, Pehlivan D, Ramocki MB, Fang P, Alleva B, Franco LM, Belmont JW, Hastings PJ, Lupski JR (2013) Replicative mechanisms for CNV formation are error prone. *Nat Genet* 45: 1319–1326
- Chen X, Cui D, Papusha A, Zhang X, Chu CD, Tang J, Chen K, Pan X, Ira G (2012) The Fun30 nucleosome remodeler promotes resection of DNA double-strand break ends. *Nature* 489: 576–580
- Church GM, Gilbert W (1984) Genomic sequencing. *Proc Natl Acad Sci USA* 81: 1991–1995
- Costantino L, Sotiriou SK, Rantala JK, Magin S, Mladenov E, Helleday T, Haber JE, Iliakis G, Kallioniemi OP, Halazonetis TD (2013) Break-induced replication repair of damaged forks induces genomic duplications in human cells. *Science* 343: 88–91
- Davis AP, Symington LS (2001) The yeast recombinational repair protein Rad59 interacts with Rad52 and stimulates single-strand annealing. *Genetics* 159: 515–525
- Deem A, Barker K, Vanhulle K, Downing B, Vayl A, Malkova A (2008) Defective break-induced replication leads to half-crossovers in *Saccharomyces cerevisiae*. *Genetics* 179: 1845–1860
- Deem A, Keszthelyi A, Blackgrove T, Vayl A, Coffey B, Mathur R, Chabes A, Malkova A (2011) Break-induced replication is highly inaccurate. *PLoS Biol* 9: e1000594
- Donnianni RA, Symington LS (2013) Break-induced replication occurs by conservative DNA synthesis. *Proc Natl Acad Sci USA* 110: 13475–13480
- Elango R, Sheng Z, Jackson J, DeCata J, Ibrahim Y, Pham NT, Liang DH, Sakofsky CJ, Vindigni A, Lobachev KS et al (2017) Break-induced replication promotes formation of lethal joint molecules dissolved by Srs2. *Nat Commun* 8: 1790
- Gallagher DN, Pham N, Tsai AM, Janto AN, Choi J, Ira G, Haber JE (2020) A Rad51-independent pathway promotes single-strand template repair in gene editing. *PLoS Genet* 16: e1008689
- Guo X, Hum YF, Lehner K, Jinks-Robertson S (2017) Regulation of hetDNA length during mitotic double-strand break repair in yeast. *Mol Cell* 67: 539–549.e4
- Haber JE (2012) Mating-type genes and MAT switching in *Saccharomyces cerevisiae*. *Genetics* 191: 33–64
- Hall SD, Kolodner RD (1994) Homologous pairing and strand exchange promoted by the *Escherichia coli* RecT protein. *Proc Natl Acad Sci USA* 91: 3205–3209
- Hastings PJ, Ira G, Lupski JR (2009) A microhomology-mediated break-induced replication model for the origin of human copy number variation. *PLoS Genet* 5: e1000327
- Hicks WM, Kim M, Haber JE (2010) Increased mutagenesis and unique mutation signature associated with mitotic gene conversion. *Science* 329: 82–85
- Holsclaw JK, Sekelsky J (2017) Annealing of complementary DNA sequences during double-strand break repair in drosophila is mediated by the ortholog of SMARCAL1. *Genetics* 206: 467–480
- Ira G, Malkova A, Liberi G, Foiani M, Haber JE (2003) Srs2 and Sgs1-Top3 suppress crossovers during double-strand break repair in yeast. *Cell* 115: 401–411
- Ira G, Satory D, Haber JE (2006) Conservative inheritance of newly synthesized DNA in double-strand break-induced gene conversion. *Mol Cell Biol* 26: 9424–9429
- Ivanov EL, Sugawara N, Fishman-Lobell J, Haber JE (1996) Genetic requirements for the single-strand annealing pathway of double-strand break repair in *Saccharomyces cerevisiae*. *Genetics* 142: 693–704
- Jain S, Sugawara N, Haber JE (2016a) Role of double-strand break end-tethering during gene conversion in *Saccharomyces cerevisiae*. *PLoS Genet* 12: e1005976
- Jain S, Sugawara N, Mehta A, Ryu T, Haber JE (2016b) Sgs1 and Mph1 helicases enforce the recombination execution checkpoint during DNA double-strand break repair in *Saccharomyces cerevisiae*. *Genetics* 203: 667–675
- Kaye JA, Melo JA, Cheung SK, Vaze MB, Haber JE, Toczyski DP (2004) DNA breaks promote genomic instability by impeding proper chromosome segregation. *Curr Biol* 14: 2096–2106
- Lao JP, Oh SD, Shinohara M, Shinohara A, Hunter N (2008) Rad52 promotes postinvasion steps of meiotic double-strand-break repair. *Mol Cell* 29: 517–524
- Lee JA, Carvalho CM, Lupski JR (2007) A DNA replication mechanism for generating nonrecurrent rearrangements associated with genomic disorders. *Cell* 131: 1235–1247
- Lee JJ, Lee J, Lee H (2020) Alternative paths to telomere elongation. *Semin Cell Dev Biol* <https://doi.org/10.1016/j.semcdb.2020.11.003>
- Lee SE, Moore JK, Holmes A, Umezū K, Kolodner RD, Haber JE (1998) *Saccharomyces* Ku70, mre11/rad50 and RPA proteins regulate adaptation to G2/M arrest after DNA damage. *Cell* 94: 399–409
- Li S, Wang H, Jehi S, Li J, Liu S, Wang Z, Truong L, Chiba T, Wang Z, Wu X (2021) PIF1 helicase promotes break-induced replication in mammalian cells. *EMBO J* 40: e104509
- Li Y, Roberts ND, Wala JA, Shapira O, Schumacher SE, Kumar K, Khurana E, Waszak S, Korbel JO, Haber JE et al (2020) Patterns of somatic structural variation in human cancer genomes. *Nature* 578: 112–121
- Li Z, Karakousis G, Chiu SK, Reddy G, Radding CM (1998) The beta protein of phage lambda promotes strand exchange. *J Mol Biol* 276: 733–744
- Liu J, Ede C, Wright WD, Gore SK, Jenkins SS, Freudenthal BD, Todd Washington M, Veaute X, Heyer WD (2017) Srs2 promotes synthesis-dependent strand annealing by disrupting DNA polymerase delta-extending D-loops. *Elife* 6: 1–24
- Liu L, Yan Z, Osia BA, Twarowski J, Sun L, Kramara J, Lee SL, Kumar S, Elango R, Li H et al (2021) Tracking break-induced replication shows that it stalls at roadblocks. *Nature* 590: 655–659
- Lobachev K, Vitriol E, Stemple J, Resnick MA, Bloom K (2004) Chromosome fragmentation after induction of a double-strand break is an active process prevented by the RMX repair complex. *Curr Biol* 14: 2107–2112
- Luke-Glaser S, Luke B (2012) The Mph1 helicase can promote telomere uncapping and premature senescence in budding yeast. *PLoS One* 7: e42028
- Lydeard JR, Jain S, Yamaguchi M, Haber JE (2007) Break-induced replication and telomerase-independent telomere maintenance require Pol32. *Nature* 448: 820–823
- Macheret M, Bhowmick R, Sobkowiak K, Padayachy L, Mailler J, Hickson ID, Halazonetis TD (2020) High-resolution mapping of mitotic DNA synthesis regions and common fragile sites in the human genome through direct sequencing. *Cell Res* 30: 997–1008
- Malkova A, Naylor ML, Yamaguchi M, Ira G, Haber JE (2005) RAD51-dependent break-induced replication differs in kinetics and checkpoint responses from RAD51-mediated gene conversion. *Mol Cell Biol* 25: 933–944
- Maloisel L, Fabre F, Gangloff S (2008) DNA polymerase delta is preferentially recruited during homologous recombination to promote heteroduplex DNA extension. *Mol Cell Biol* 28: 1373–1382

- Mayle R, Langston L, Molloy KR, Zhang D, Chait BT, O'Donnell ME (2019) Mcm10 has potent strand-annealing activity and limits translocase-mediated fork regression. *Proc Natl Acad Sci USA* 116: 798–803
- Mazloum N, Holloman WK (2009) Second-end capture in DNA double-strand break repair promoted by Brh2 protein of *Ustilago maydis*. *Mol Cell* 33: 160–170
- McGill C, Shafer B, Strathern J (1989) Coconversion of flanking sequences with homothallic switching. *Cell* 57: 459–467
- McIlwraith MJ, Vaisman A, Liu Y, Fanning E, Woodgate R, West SC (2005) Human DNA polymerase  $\eta$  promotes DNA synthesis from strand invasion intermediates of homologous recombination. *Mol Cell* 20: 783–792
- McIlwraith MJ, West SC (2008) DNA repair synthesis facilitates RAD52-mediated second-end capture during DSB repair. *Mol Cell* 29: 510–516
- McPherson JP, Lemmers B, Chahwan R, Pamidi A, Migon E, Matysiak-Zablocki E, Moynahan ME, Essers J, Hanada K, Poonepalli A et al (2004) Involvement of mammalian Mus81 in genome integrity and tumor suppression. *Science* 304: 1822–1826
- Mehta A, Beach A, Haber JE (2017) Homology requirements and competition between gene conversion and break-induced replication during double-strand break repair. *Mol Cell* 65: 515–526: e513
- Mimitou EP, Symington LS (2010) Ku prevents Exo1 and Sgs1-dependent resection of DNA ends in the absence of a functional MRX complex or Sae2. *EMBO J* 29: 3358–3369
- Mitchel K, Lehner K, Jinks-Robertson S (2013) Heteroduplex DNA position defines the roles of the Sgs1, Srs2, and Mph1 helicases in promoting distinct recombination outcomes. *PLoS Genet* 9: e1003340
- Mortensen UH, Bendixen C, Sunjevaric I, Rothstein R (1996) DNA strand annealing is promoted by the yeast Rad52 protein. *Proc Natl Acad Sci USA* 93: 10729–10734
- Mortensen UH, Erdeniz N, Feng Q, Rothstein R (2002) A molecular genetic dissection of the evolutionarily conserved N terminus of yeast Rad52. *Genetics* 161: 549–562
- Nimonkar AV, Sica RA, Kowalczykowski SC (2009) Rad52 promotes second-end DNA capture in double-stranded break repair to form complement-stabilized joint molecules. *Proc Natl Acad Sci USA* 106: 3077–3082
- Oh J, Lee SJ, Rothstein R, Symington LS (2018) Xrs2 and Tel1 independently contribute to MR-mediated DNA tethering and replisome stability. *Cell Rep* 25: 1681–1692.e4
- Osman F, Dixon J, Barr AR, Whitby MC (2005) The F-Box DNA helicase Fbh1 prevents Rhp51-dependent recombination without mediator proteins. *Mol Cell Biol* 25: 8084–8096
- Ozenberger BA, Roeder GS (1991) A unique pathway of double-strand break repair operates in tandemly repeated genes. *Mol Cell Biol* 11: 1222–1231
- Petukhova G, Stratton SA, Sung P (1999) Single strand DNA binding and annealing activities in the yeast recombination factor Rad59. *J Biol Chem* 274: 33839–33842
- Piazza A, Shah SS, Wright WD, Gore SK, Koszul R, Heyer WD (2019) Dynamic processing of displacement loops during recombinational DNA repair. *Mol Cell* 73: 1255–1266.e4
- Ponder RG, Fonville NC, Rosenberg SM (2005) A switch from high-fidelity to error-prone DNA double-strand break repair underlies stress-induced mutation. *Mol Cell* 19: 791–804
- Prakash R, Satory D, Dray E, Papusha A, Scheller J, Kramer W, Krejci L, Klein H, Haber JE, Sung P et al (2009) Yeast Mph1 helicase dissociates Rad51-made D-loops: implications for crossover control in mitotic recombination. *Genes Dev* 23: 67–79
- Robert T, Dervins D, Fabre F, Gangloff S (2006) Mrc1 and Srs2 are major actors in the regulation of spontaneous crossover. *EMBO J* 25: 2837–2846
- Roumelioti FM, Sotiriou SK, Katsini V, Chiourea M, Halazonetis TD, Gagos S (2016) Alternative lengthening of human telomeres is a conservative DNA replication process with features of break-induced replication. *EMBO Rep* 17: 1731–1737
- Saini N, Ramakrishnan S, Elango R, Ayyar S, Zhang Y, Deem A, Ira G, Haber JE, Lobachev KS, Malkova A (2013) Migrating bubble during break-induced replication drives conservative DNA synthesis. *Nature* 502: 389–392
- Sakofsky CJ, Ayyar S, Deem AK, Chung WH, Ira G, Malkova A (2015) Translesion polymerases drive microhomology-mediated break-induced replication leading to complex chromosomal rearrangements. *Mol Cell* 60: 860–872
- Sakofsky CJ, Malkova A (2017) Break induced replication in eukaryotes: mechanisms, functions, and consequences. *Crit Rev Biochem Mol Biol* 52: 395–413
- Sakofsky CJ, Roberts SA, Malc E, Mieczkowski PA, Resnick MA, Gordenin DA, Malkova A (2014) Break-induced replication is a source of mutation clusters underlying kataegis. *Cell Rep* 7: 1640–1648
- Shcherbakova PV, Pavlov YI (1996) 3'→5' exonucleases of DNA polymerases epsilon and delta correct base analog induced DNA replication errors on opposite DNA strands in *Saccharomyces cerevisiae*. *Genetics* 142: 717–726
- Shee C, Gibson JL, Rosenberg SM (2012) Two mechanisms produce mutation hotspots at DNA breaks in *Escherichia coli*. *Cell Rep* 2: 714–721
- Shi I, Hallwyl SC, Seong C, Mortensen U, Rothstein R, Sung P (2009) Role of the Rad52 amino-terminal DNA binding activity in DNA strand capture in homologous recombination. *J Biol Chem* 284: 33275–33284
- Shim EY, Chung WH, Nicolette ML, Zhang Y, Davis M, Zhu Z, Paull TT, Ira G, Lee SE (2010) *Saccharomyces cerevisiae* Mre11/Rad50/Xrs2 and Ku proteins regulate association of Exo1 and Dna2 with DNA breaks. *EMBO J* 29: 3370–3380
- Smith CE, Llorente B, Symington LS (2007) Template switching during break-induced replication. *Nature* 447: 102–105
- Smith DJ, Whitehouse I (2012) Intrinsic coupling of lagging-strand synthesis to chromatin assembly. *Nature* 483: 434–438
- Stafa A, Donnianni RA, Timashev LA, Lam AF, Symington LS (2014) Template switching during break-induced replication is promoted by the Mph1 helicase in *Saccharomyces cerevisiae*. *Genetics* 196: 1017–1028
- Stivison EA, Young KJ, Symington LS (2020) Interstitial telomere sequences disrupt break-induced replication and drive formation of ectopic telomeres. *Nucleic Acids Res* 48: 12697–12710
- Sugawara N, Ira G, Haber JE (2000) DNA length dependence of the single-strand annealing pathway and the role of *Saccharomyces cerevisiae* RAD59 in double-strand break repair. *Mol Cell Biol* 20: 5300–5309
- Sugiyama T, Kantake N, Wu Y, Kowalczykowski SC (2006) Rad52-mediated DNA annealing after Rad51-mediated DNA strand exchange promotes second ssDNA capture. *EMBO J* 25: 5539–5548
- Sugiyama T, New JH, Kowalczykowski SC (1998) DNA annealing by RAD52 protein is stimulated by specific interaction with the complex of replication protein A and single-stranded DNA. *Proc Natl Acad Sci USA* 95: 6049–6054
- Sun W, Nandi S, Osman F, Ahn JS, Jakovleska J, Lorenz A, Whitby MC (2008) The FANCM ortholog Fml1 promotes recombination at stalled replication forks and limits crossing over during DNA double-strand break repair. *Mol Cell* 32: 118–128
- Symington LS (2016) Mechanism and regulation of DNA end resection in eukaryotes. *Crit Rev Biochem Mol Biol* 51: 195–212

- Symington LS, Rothstein R, Lisby M (2014) Mechanisms and regulation of mitotic recombination in *Saccharomyces cerevisiae*. *Genetics* 198: 795–835
- Valencia-Burton M, Oki M, Johnson J, Seier TA, Kamakaka R, Haber JE (2006) Different mating-type-regulated genes affect the DNA repair defects of *Saccharomyces* RAD51, RAD52 and RAD55 mutants. *Genetics* 174: 41–55
- Weiss K, Simpson RT (1998) High-resolution structural analysis of chromatin at specific loci: *Saccharomyces cerevisiae* silent mating type locus HMLalpha. *Mol Cell Biol* 18: 5392–5403
- Westmoreland J, Ma W, Yan Y, Van Hulle K, Malkova A, Resnick MA (2009) RAD50 is required for efficient initiation of resection and recombinational repair at random, gamma-induced double-strand break ends. *PLoS Genet* 5: e1000656
- Westmoreland JW, Resnick MA (2013) Coincident resection at both ends of random, gamma-induced double-strand breaks requires MRX (MRN), Sae2 (Ctp1), and Mre11-nuclease. *PLoS Genet* 9: e1003420
- Wilson MA, Kwon Y, Xu Y, Chung WH, Chi P, Niu H, Mayle R, Chen X, Malkova A, Sung P et al (2013) Pif1 helicase and Poldelta promote recombination-coupled DNA synthesis via bubble migration. *Nature* 502: 393–396
- Wu X, Haber JE (1996) A 700 bp cis-acting region controls mating-type dependent recombination along the entire left arm of yeast chromosome III. *Cell* 87: 277–285
- Wu Y, Kantake N, Sugiyama T, Kowalczykowski SC (2008) Rad51 protein controls Rad52-mediated DNA annealing. *J Biol Chem* 283: 14883–14892
- Wu Y, Sugiyama T, Kowalczykowski SC (2006) DNA annealing mediated by Rad52 and Rad59 proteins. *J Biol Chem* 281: 15441–15449
- Yan Z, Xue C, Kumar S, Crickard JB, Yu Y, Wang W, Pham N, Li Y, Niu H, Sung P et al (2019) Rad52 restrains resection at DNA double strand break ends in yeast. *Mol Cell* 76: 699–711.e6
- Zhu Z, Chung WH, Shim EY, Lee SE, Ira G (2008) Sgs1 helicase and two nucleases dna2 and exo1 resect DNA double-strand break ends. *Cell* 134: 981–994